

Tx-LLM: A Large Language Model for Therapeutics

Juan Manuel Zambrano Chaves^{*,1}, Eric Wang^{*,2}, Tao Tu², Eeshit Dhaval Vaishnav,
Byron Lee, S. Sara Mahdavi², Christopher Semturs¹, David Fleet²,
Vivek Natarajan^{†,1} and Shekoofeh Azizi^{†,‡,2}

¹Google Research, ²Google DeepMind

Developing therapeutics is a lengthy and expensive process that requires the satisfaction of many different criteria, and AI models capable of expediting the process would be invaluable. However, the majority of current AI approaches address only a narrowly defined set of tasks, often circumscribed within a particular domain. To bridge this gap, we introduce Tx-LLM, a generalist large language model (LLM) fine-tuned from PaLM-2 which encodes knowledge about diverse therapeutic modalities. Tx-LLM is trained using a collection of 709 datasets that target 66 tasks spanning various stages of the drug discovery pipeline. Using a single set of weights, Tx-LLM simultaneously processes a wide variety of chemical or biological entities (small molecules, proteins, nucleic acids, cell lines, diseases) interleaved with free-text, allowing it to predict a broad range of associated properties, achieving competitive with state-of-the-art (SOTA) performance on 43 out of 66 tasks and exceeding SOTA on 22. Among these, Tx-LLM is particularly powerful and exceeds best-in-class performance on average for tasks combining molecular SMILES representations with text such as cell line names or disease names, likely due to context learned during pretraining. We observe evidence of positive transfer between tasks with diverse drug types (*e.g.*, tasks involving small molecules and tasks involving proteins), and we study the impact of model size, domain finetuning, and prompting strategies on performance. We believe Tx-LLM represents an important step towards LLMs encoding biochemical knowledge and could have a future role as an end-to-end tool across the drug discovery development pipeline.

1 Introduction

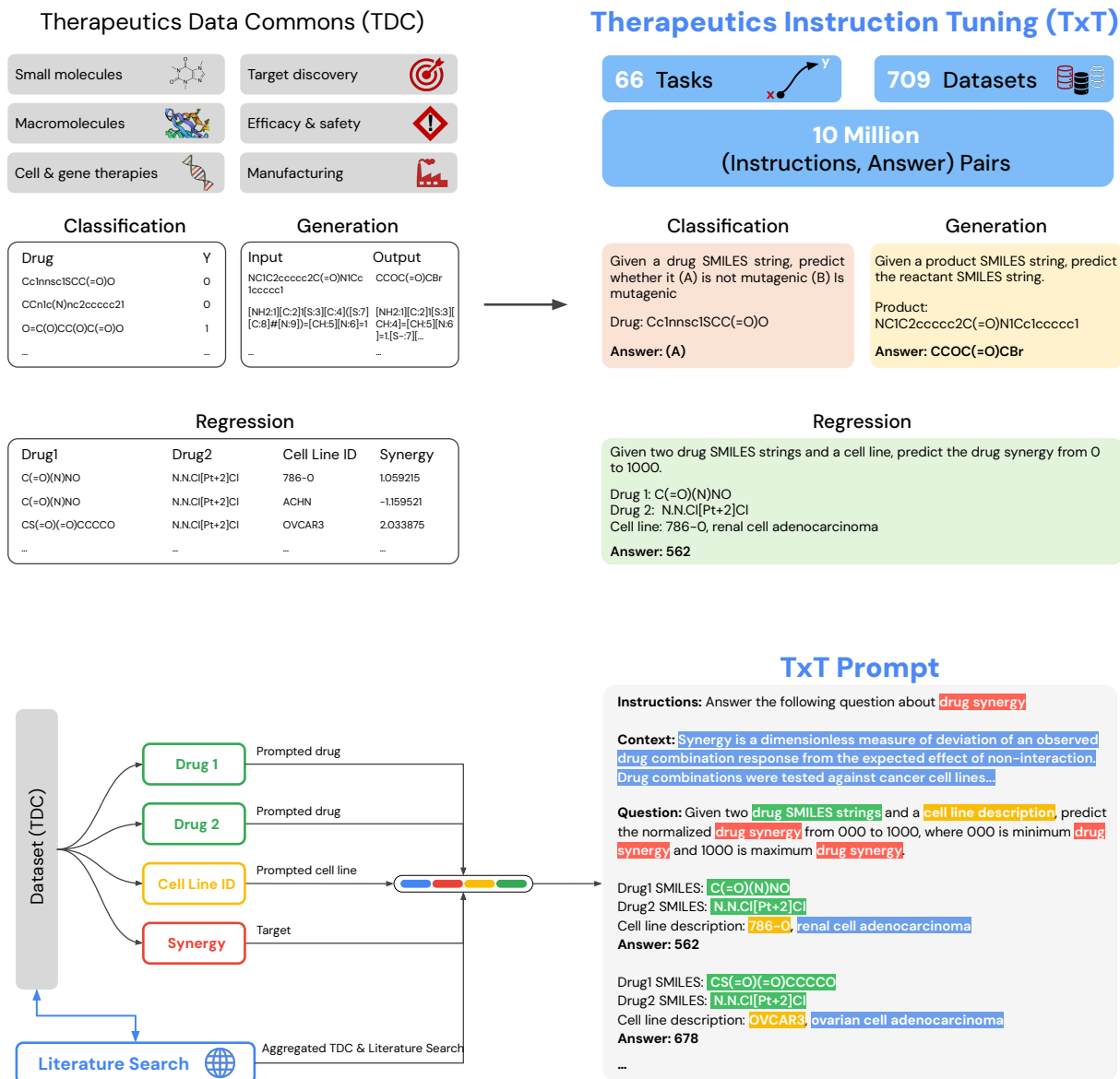
Developing therapeutics is a risky enterprise, as 90% of clinical trial candidates fail, and even successful therapeutics typically take 10-15 years and 1-2 billion dollars until approval [1, 2]. Perhaps the most daunting obstacle in this process is that a successful therapeutic must simultaneously satisfy numerous criteria. For example, a drug should interact with its proposed target, ultimately leading to the desired therapeutic effect and clinical efficacy. At the same time, the drug should be non-toxic and have drug-like properties (*e.g.*, solubility, permeability, suitable pharmacokinetics, and pharmacodynamics). In clinical trials, unexpected off-target effects and interactions may counterbalance the effects of an otherwise promising drug candidate [3]. Furthermore, practical considerations regarding small molecule synthesis, or biological molecule developability must be taken into account.

Given the expense of experimentally assessing each of these characteristics, curated collections of experimental data paired with machine learning models for predicting therapeutic properties are useful as initial screening steps [4]. To aid the development of these models, the Therapeutics Data Commons (TDC) was developed as a resource containing AI-ready datasets and benchmarks for a diverse range of therapeutics-related tasks such as drug-target binding prediction or drug toxicity prediction [5, 6]. Current state-of-the-art (SOTA) models for TDC datasets are largely focused on individual tasks with one approach being to train a library of specialist models and call upon different specialists for each step of the therapeutic development pipeline [5]. However, specialist models lack awareness of other tasks in the therapeutic development pipeline, which may in turn limit their ability to contextualize and improve performance.

Large language models (LLMs) have emerged as useful systems for encoding information from large-scale data

* Equal contributions. Contributions made as a student researcher. † Equal leadership.

‡ Corresponding author: shekazizi@google.com



Instructions: Answer the following question about **drug synergy**

Context: Synergy is a dimensionless measure of deviation of an observed drug combination response from the expected effect of non-interaction. Drug combinations were tested against cancer cell lines...

Question: Given two **drug SMILES strings** and a **cell line description**, predict the normalized **drug synergy** from 000 to 1000, where 000 is minimum **drug synergy** and 1000 is maximum **drug synergy**.

Drug1 SMILES: C(=O)(N)NO
Drug2 SMILES: N.N.C[Pt+2]Cl
Cell line description: 786-O, renal cell adenocarcinoma

Answer: 562

Drug1 SMILES: CS(=O)(=O)CCCCO
Drug2 SMILES: N.N.C[Pt+2]Cl
Cell line description: OVCAR3, ovarian cell adenocarcinoma

Answer: 678

...

Figure 1 | Overview of the Tx-LLM. (top) Datasets from the Therapeutic Data Commons are used to construct the Therapeutics instruction Tuning (TxT) collection. The original tabular datasets contain a variety of drug types including small molecules, macro-molecules such as proteins and nucleic acids, cells, and genes. The tasks encompass a broad range of areas relevant to drug discovery and development such as predicting targets, evaluating efficacy and safety, and predicting ease of manufacturing. TxT interleaves free-text instructions with string representations of molecules, such as SMILES strings for small molecules or amino acid sequences for proteins. TxT is used to prompt and finetune Tx-LLM to solve classification, regression, or generation tasks. **(bottom)** Example of a TxT prompt for predicting drug synergy. The prompt is composed of Instructions, Context, and a Question using information from the corresponding TDC dataset and/or literature search and may also contain exemplars to aid in-context learning.

and communicating the information using language. Interestingly, LLMs have shown promise for multiple types of tasks such as multiple-choice question answering [7], time series prediction [8], and regression [9]. Furthermore, LLMs can be effectively adapted to specific domains such as medicine or chemistry with in-context learning or finetuning [10–14]. We hypothesized that tasks across the therapeutic development pipeline, even those involving diverse drug types such as small molecules and protein sequences, could be combined to train a generalist LLM with improved performance on individual tasks while using the same set of weights for all tasks.

In this work, we develop and introduce such a generalist model, Tx-LLM, by representing therapeutics as strings and finetuning the PaLM-2 base LLM on a diverse set of classification, regression, and generation tasks (Figure 1). Our key contributions are as follows:

- Tx-LLM performs above or near SOTA for 43 out of 66 tasks. For datasets combining molecular string representations with text, Tx-LLM is especially effective and exceeds SOTA on average for these, likely due to context learned during LLM pretraining.
- Interestingly, we find evidence of positive transfer between datasets with diverse drug types, as training on datasets including biological sequences improves performances on molecular datasets.
- We perform ablation studies and observe that scale, domain finetuning, and prompting strategies also significantly impact model performance.
- The proposed Tx-LLM shows promise as an end-to-end therapeutic development assist, allowing one to query a single model for multiple steps of the development pipeline (Figure 2).

2 Related works

Large language models (LLMs) Since the advent of transformer-based models [15], LLMs have become increasingly powerful at a variety of natural language processing tasks [16, 17]. LLMs are trained using self-supervised learning on large-scale text corpora and have been shown to encode information while also generalizing to unseen tasks. Interestingly, it has recently been shown that LLMs are able to perform regression on diverse tasks using only textual representations of mathematical parameters and values [9].

Specialist models for therapeutics Therapeutics have been represented in a variety of ways. Molecules can be naturally represented as graphs, and graph neural networks (GNNs) have been applied for a variety of prediction or generation tasks [18–24]. A notable application of GNNs was the discovery of Halicin, an antibiotic which was effective against previously pan-resistant bacterial strains [25]. Molecules are also commonly represented using binary vectors (fingerprints), which capture the local environment of each atom in the molecule within a predefined radius and can be input into a variety of models [26–28]. Proteins and nucleic acids are conveniently represented using their amino acid or nucleotide sequences, and which can then be encoded in multiple ways to predict properties such as fitness [29], binding [30, 31], and secondary structure [32]. The introduction of AlphaFold and its successors significantly advanced the field of structure prediction [33–36], which may allow further developments in areas such as design of structure-based drugs [37] and vaccines [38].

Language models for biology and chemistry Language models have also emerged as tools for biology and chemistry. While many LLMs have shown limited performance for chemistry [39, 40], LlaSMol recently showed that finetuning LLMs for chemistry achieved near-SOTA performance on multiple tasks [41]. Beyond chemical property prediction, Chemcrow used LLMs for robotics-guided organic synthesis without human interaction [42]. Protein language models such as ESM [43, 44], Unirep [45], and ProtGPT2 [46] have used self-supervised pretraining (such as masked token prediction) to generate protein embeddings that were useful for downstream tasks such as predicting stability and functional effects of mutations. It has also been proposed that the probabilities assigned to amino acids during masked token prediction correlate to fitness [47] and provide an efficient landscape for computational protein engineering [48]. ProtLLM combined protein sequence encoders with language encoders [49], and BioT5 combined molecular string representations with protein names, sequences, or structures to train LLMs on various prediction tasks [50]. At the cellular level, scGPT [51], GenePT [52], and Geneformer [53] represent cells as rank ordered lists of highly expressed genes for tasks such as cell type annotation or therapeutic target discovery.

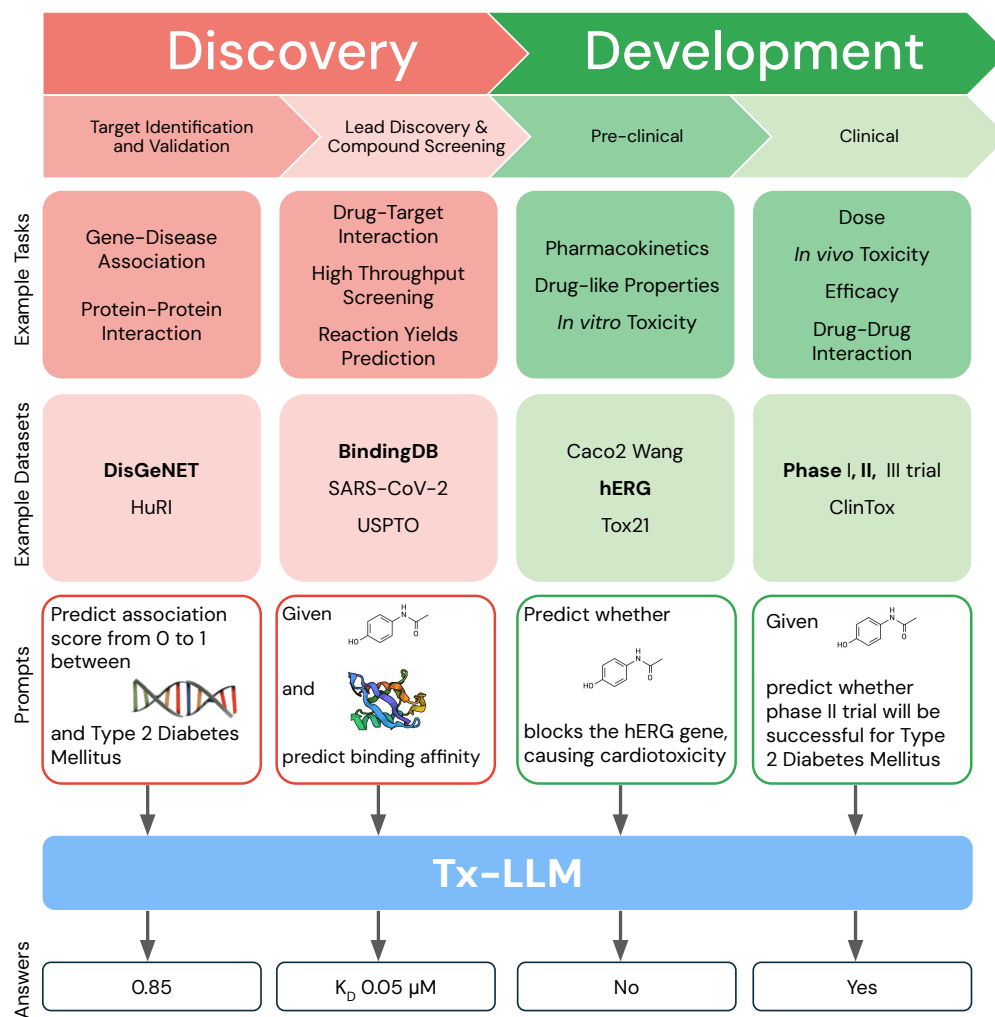


Figure 2 | Tx-LLM may be effective for end-to-end therapeutic development. Tx-LLM is a single model that can be queried for multiple steps of the therapeutic development process, covering tasks from early-stage target discovery to late-stage clinical trial approval. We list example tasks associated with each stage of the therapeutic development pipeline, example datasets in TDC that correspond to these tasks, and example prompts that can be used to query Tx-LLM. For illustration, the example prompts are geared towards discovering new small molecules against targets associated with type 2 diabetes, and the datasets associated with the example prompts are shown in bold.

3 Methods

3.1 Datasets

We assembled TxT, a collection of 709 drug discovery datasets comprising 66 tasks formatted for instruction tuning. We sourced our datasets from TDC, a publicly available repository that offers a wide variety of tasks spanning the drug discovery process. The median dataset size was 11,000, and the distribution of dataset sizes is illustrated in Figure A.1. We excluded a small number of datasets found in TDC for various reasons, which are detailed in Table A.1.

Each dataset in TxT is formatted as a text prompt comprised of four components (instructions, context, question, answer), illustrated in Figure 1 and Tables A.3 to A.5. Instructions consisted of a short sentence describing the task at hand, such as “Answer the following question about drug properties”. For each dataset, we crafted context, *i.e.*, free-text descriptions providing additional information that grounds the question in a relevant biochemical setting. Contexts were 2-3 sentences long, sourced from TDC dataset descriptions, and manually complemented based on a brief literature search of the topic. For specialized assays describing a specific experimental condition, such as ToxCast, additional information for contexts were obtained from publicly available assay descriptions [54, 55]. The question is a succinct query that specifies the specific property being asked, and interleaves English text with text-based representations of therapeutics (*e.g.*, “Does the following molecule cross the blood brain barrier? <molecule>”). The format of answers varied depending of the type of task.

Datasets in TxT fell into one of three categories:

- (i) **Binary classification** questions were formatted as a prediction of a single property of a therapeutic with two possibilities, yes/no (*e.g.*, whether a drug is toxic).
- (ii) **Regression** questions were formatted as a prediction of a single property of a therapeutic on a continuous scale (e.g. drug-target binding affinity). To leverage the token-based, and not float-based, representation in existing language models, we uniformly binned the labels between 0 and 1000 and instruct Tx-LLM to predict the bin label. On evaluation, the predicted bin was transformed back to the original numeric label space.
- (iii) **Generation** we focused on one generation task, which consists of predicting reactants of a chemical reaction given the product, sourced from the USPTO dataset [56].

String representations of diverse types of therapeutics in TxT fell into one of the following categories:

- (i) **SMILES** Small molecules were represented with their SMILES string.
- (ii) **Amino acid** Proteins and peptides were represented with their amino acid sequences. Multiple Histopatibility Complex molecules, such as those found in the in the MHC1 IEDB IMGT Nielsen [57] and MHC2 IEDB Jensen [58] datasets were represented using their pseudo-sequences (only showing residues that are in contact with a peptide), T cell receptors were represented using their CDR3 hypervariable loops.
- (iii) **Nucleotide** Nucleic acids were represented with their nucleotide sequence.
- (iv) **Amino acid + SMILES** Multi-instance datasets containing both proteins and small molecules used the protein amino acid sequence and the molecular SMILES string.
- (v) **Nucleotide + Amino acid** Multi-instance datasets containing both nucleic acids and proteins used the nucleotide sequence and protein amino acid sequence.
- (vi) **SMILES + Text** Multi-instance datasets containing small molecules and other feature types used the molecular SMILES string and English text to represent the additional features, such as disease or cell line names and descriptions. Notable datasets in this category include Phase I, Phase II, and Phase III clinical trial datasets. These datasets contain information about the SMILES strings of candidate drugs, the names of targeted diseases for various clinical trial phases, and whether the trial ultimately received approval.
- (vii) **Amino acid + Text** Multi-instance datasets containing proteins and other feature types used the protein amino acid sequence and text to represent the other features. DisGeNET, which contained protein sequences and disease names, was the only dataset in this category.

For each dataset, data splits were constructed using TDC functions with recommended split methods (random, scaffold, cold-start, combination, temporal), which are indicated in Tables A.7 and A.8. For datasets in the ADMET, DrugCombo, or DTI DG leaderboards, we followed the leaderboard-specific instructions for generating splits with a seed of 1.

3.2 Modeling

Base LLM Tx-LLM was initiated from PaLM-2 [59], the second generation of Google’s LLM trained using the Pathways accelerator orchestration system [60]. PaLM-2 models used in this work were trained at sizes S and M.

Few-shot prompting Few-shot prompting [16] involves providing example inputs and outputs in the prompt. Based on prior evidence showing the benefits of using a mixture of 0 and few-shot tasks [61], we constructed TxT as a mixture of 70% 0-shot and 30% few-shot prompts with the number of few shots randomly chosen between 1 and 10. If the shots caused the prompt to exceed the maximum length, then the number of shots was reduced until the length was below the maximum. The shots were selected using random datapoints in the training dataset. On evaluation, we also considered nearest neighbor shots, but we strictly used random shots during training because the datapoints were often more similar within the training set than across training and test sets (Figure A.2).

Finetuning We finetuned a non-instruction tuned variant of PaLM-2 using TxT training data. We trained a single model across all TDC datasets using dataset mixture ratios proportional to the number of datapoints in each dataset. Tx-LLM generally refers to Tx-LLM (M) models trained across all TDC datasets. We explored various key ablations using subsets of TDC datasets for comparison using a smaller, Tx-LLM (S) due to constraints on computational resources. Hyperparameters for finetuning are listed in Table A.2.

3.3 Evaluation

State-of-the-art performance SOTA values reported in this work are primarily derived from academic literature. For TDC datasets included in the ADMET, DrugCombo, and DTI DG leaderboards, SOTA values were obtained directly from the respective leaderboard. For datasets not featured in a leaderboard, SOTA values were determined through a manual literature review.

Few-shot prompting We evaluated the performance of Tx-LLM with 0 and few-shot prompting, varying the number of shots and whether the shots were selected based on random datapoints or nearest neighbor datapoints. Nearest neighbors were identified using representations of the query therapeutic(s). For small molecules, nearest neighbors were identified using Tanimoto similarities with Morgan fingerprints, whereas for amino acid and nucleotide sequences percent sequence identities were used. Morgan fingerprints and Tanimoto similarities were calculated using RDKit and Chemfp [62, 63], and multiple sequence alignments for percent sequence identities were calculated using Clustal Omega [64]. For validation, shots were selected from the training sets, whereas shots for test sets were selected from the combined training and validation sets.

Metrics We report Tx-LLM performances on TDC datasets using the preferred metric for each task as defined by [6]. Metrics for binary classification datasets include area under the receiver operating characteristic curve (AUROC), area under the precision-recall curve (AUPRC), and accuracy. Metrics for regression datasets include the Spearman correlation coefficient, Pearson correlation coefficient, mean absolute error (MAE), and mean squared error (MSE). The metric for the USPTO generation dataset is set accuracy, where for each reaction set overlaps between the generated reactants compared to the ground-truth reactants were assigned a score of 1 if there was perfect overlap, and 0 otherwise.

Statistical tests Given performances on TDC datasets from two models, we sought to determine whether one model was significantly better considering all datasets. To do this, we performed a non-parametric Wilcoxon signed-rank test on the performances from both models and report the p-value. In order to account for the differences in magnitudes for MAE and MSE metrics, we normalized all performances by the mean of the performances from both models. We also reversed the sign of MAEs and MSEs because lower MAEs and MSEs correspond to better performances.

Data contamination analysis PaLM-2 was trained on diverse data [59] that may contain information about

therapeutics in TDC. To study this, we analyzed the percent overlap between TDC dataset features and the PaLM-2 training data. To illustrate an example, consider the case of a TDC dataset containing SMILES strings for molecules paired with target amino acid sequences. For each TDC datapoint, two searches over the PaLM-2 training data were performed using (i) the full SMILES string and (ii) the full amino acid sequence, and the datapoint was considered overlapping if either the SMILES string or amino acid sequence were found in the PaLM-2 training data. The minimum match length was set to the SMILES/amino acid sequence length, up to a maximum of 512 characters due to infrastructural constraints. Our analysis looks for direct character overlaps and does not account for different representations of the same feature, such as molecules being represented as SMILES strings in TDC but being referred to by name in the PaLM-2 training data.

4 Results

4.1 Performance on TDC datasets

The performance of Tx-LLM on TDC datasets is summarized in Figure 3 and Tables A.7 and A.8. Out of 66 TDC tasks, Tx-LLM performed near or exceeding SOTA on 43 datasets. From these 43 datasets, Tx-LLM outperformed SOTA on 22 (12 binary classification datasets and 10 regression datasets) and performed near SOTA (defined as within 10% of SOTA) for another 21 (12 binary classification datasets and 9 regression datasets). Notably, these results were achieved using the same set of model weights without any task-specific optimizations.

Tx-LLM is particularly effective at combining SMILES and text TDC datasets containing features involving SMILES strings for molecules and text for other features (such as disease name or cell line name and description) tended to perform near or exceeding SOTA more frequently than datasets containing other features types (Figure 3 and Tables A.7 and A.8). To quantify this trend, we calculated the median relative difference of Tx-LLM performance from SOTA (defined as $(\text{Tx-LLM performance} - \text{SOTA}) / \text{SOTA}$) for each feature type (SMILES + Text, Nucleotide + Amino acid, SMILES, Amino acid, Amino acid + SMILES, Nucleotide) in Table A.6. In calculating the relative differences, signs were reversed for MAE and MSE metrics because lower MAEs and MSEs correspond to better performances. Amino acid + Text was not included because only the DisGeNET dataset, which we did not find a SOTA for, had this feature type.

SMILES + Text was the only feature type yielding a positive median relative difference, suggesting that it was the only feature type which tended to exceed SOTA on average. This performance may be due to the text representations for diseases and cell lines, both because text is a natural representation for a LLM and because the base LLM may have learned context about these in its pretraining. The ability to exceed SOTA may also be in part due to the difficulty in representing these features with non-LLM models. For example, SOTA models for the clinical trial approval datasets (phase 1, phase 2, and phase 3) represent diseases as nodes in an interaction graph [65], which may contain less information than context learned from LLM pretraining.

Overall, these results suggest that finetuned LLMs may be particularly effective for tasks involving both a drug and a target that can be represented in text (such as disease name or cell line name). In a sense, a finetuned LLM is an intermediate model between a domain-specific model, such as a GNN which is effective for representing molecules but less effective for other features, and a base LLM that does not understand molecular SMILES strings [39] but does contain diverse knowledge about physiology. Thus, a finetuned LLM may be an ideal model for tasks involving both.

Limitations of Tx-LLM for datasets without textual features In contrast, Tx-LLM underperformed SOTA on small molecule datasets solely using SMILES strings (Table A.6). This suggests that SOTA models representing molecules as graphs may be more effective than those relying only on SMILES strings, as SMILES strings have limitations such as non-uniqueness [66]. Additionally, LLM-generated SMILES strings may not follow proper SMILES grammar, which renders them invalid and possibly constitute hallucinations. In our work, datasets involving protein amino acid sequences perform similarly as those involving SMILES strings relative to SOTA models (Table A.6), which is less intuitive because proteins are naturally represented as sequences. One consideration is that SOTA models often encode evolutionary or structural information that is not learned by pretraining a LLM on natural language text. For example, BiComp-DTA uses evolutionary information from combining alignment-free and alignment-based methods in its protein encoding to predict

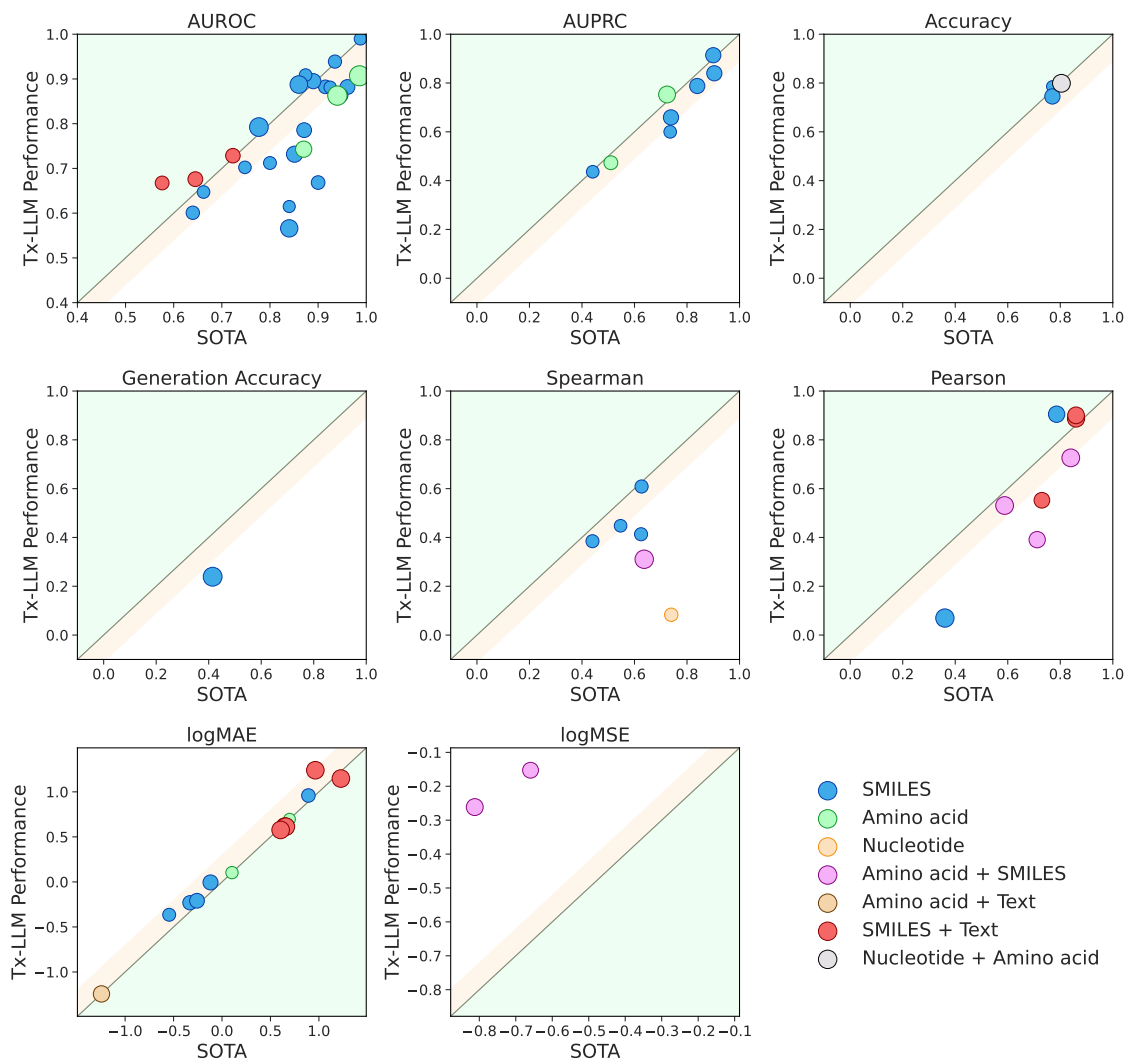


Figure 3 | Comparison of Tx-LLM's performance with SOTA. Tx-LLM is evaluated on each dataset in TDC, and comparison with SOTA for different metrics is illustrated in panels. Datasets are colored by their feature types indicated in the legend, and marker sizes illustrate the number of data points in the task on a log scale. The larger shaded area in green indicates where Tx-LLM outperforms SOTA, while the narrower orange shaded area indicates where Tx-LLM is near SOTA (defined as within 10%). MAE and MSE values are log-transformed because the magnitudes of these values depend on the units of the outputs. Generation accuracy is the fraction of correct SMILES strings in the USPTO generation task.

drug-target dissociation constants, and Kinnings *et al.* [67] perform structure-based docking calculations to predict drug-target IC_{50} s.

Evidence of data contamination affecting Tx-LLM performance was not observed We analyzed the percent overlap between TDC datasets and the PaLM-2 training data in Table A.17. The large majority of datasets do not have any overlap with the PaLM-2 training data, while 7 datasets have some overlap. For these 7 datasets, we also filter the test set to remove the overlapping datapoints, and the performances on the filtered test sets do not decrease relative to the unfiltered test sets. We caution that our contamination analysis looks for direct character overlaps and thus may miss overlapping features that are represented in different forms between the PaLM-2 training data and TDC datasets. In particular, molecules are represented as SMILES strings in TDC but likely referred to by name in natural language text used to train a generic LLM.

4.2 Evidence of positive transfer across datasets with diverse drug types

To assess positive transfer in Tx-LLM, we trained a Tx-LLM (S) model only on TDC datasets containing molecules (excluding datasets involving other drug types such as proteins and nucleic acids) and compared the performance on small molecule datasets against the Tx-LLM (S) trained on all TDC datasets. The results in Figure 4 illustrate that the model trained on all datasets performs better than the model trained on small molecule datasets when evaluated on 43 out of 56 small molecule datasets.

To determine whether this improved performance was statistically significant, we performed a Wilcoxon signed-rank test on the small molecule dataset performances from both models (see Methods). The difference in performances between the model trained on all datasets and the model trained on small molecule datasets was highly significant ($\rho = 1.4 \times 10^{-5}$), showing evidence of positive transfer between datasets involving diverse drug types and datasets involving small molecules. This is interesting given that other drug types such as proteins and nucleic acids are represented using their sequences, which are quite different from the SMILES strings used to represent small molecules. This may be because small molecules and proteins are more similar to each other than to natural language, so additional training steps away from PaLM-2 are ultimately helpful.

A model trained only on datasets in the ADMET benchmark group, which was a subset of small molecule datasets, was also evaluated in Tables A.15 and A.16 in order to study positive transfer between small molecule datasets and ADMET datasets. For datasets in the ADMET benchmark, the model trained on small molecule datasets was the best model for only 4 ADMET datasets, while the model trained on ADMET datasets was the best model for 7 ADMET datasets. Interestingly, the model trained on all datasets was the best model for 11 ADMET datasets, suggesting that positive transfer between datasets with diverse drug types may be more impactful than positive transfer within small molecule datasets. This may support the use of a generalist model that expresses many drug types with the same string representation, rather than using separate representations for each drug type.

4.3 Ablations

Model size and finetuning We compared performances on TDC datasets for models of multiple sizes (Tx-LLM (S) and Tx-LLM (M)) to examine the effect of model scale in Figures A.3 and A.4 and Tables A.9 and A.10. Additionally, we evaluated PaLM 2 (S) and PaLM 2 (M) as baseline generalist models in order to study the effect of biochemical domain finetuning. Tx-LLM (M) outperformed Tx-LLM (S) on 57 out of 66 TDC datasets, suggesting that scale is beneficial within our tested sizes ($\rho = 1.65 \times 10^{-7}$, Wilcoxon signed-rank test). Domain finetuning is also significant, as Tx-LLM outperforms PaLM-2 on 60 datasets for the S models ($\rho = 1.86 \times 10^{-10}$, Wilcoxon signed-rank test) and on 63 datasets for the M models ($\rho = 3.58 \times 10^{-11}$, Wilcoxon signed-rank test).

Number of shots and shot selection We compared varying the number of shots in the prompt as well as whether the shots are selected from random datapoints or nearest neighbor datapoints in order to study the extent to which Tx-LLM could exploit in-context learning in Figures A.3 and A.4 and Tables A.11 and A.12. We observed that the best performances were not clearly skewed toward a particular prompting strategy, and pairwise comparisons did not yield statistically significant differences ($\rho > 0.05$, Wilcoxon signed-rank test). This is consistent with previous observations that zero-shot and few-shot prompting yielded marginal

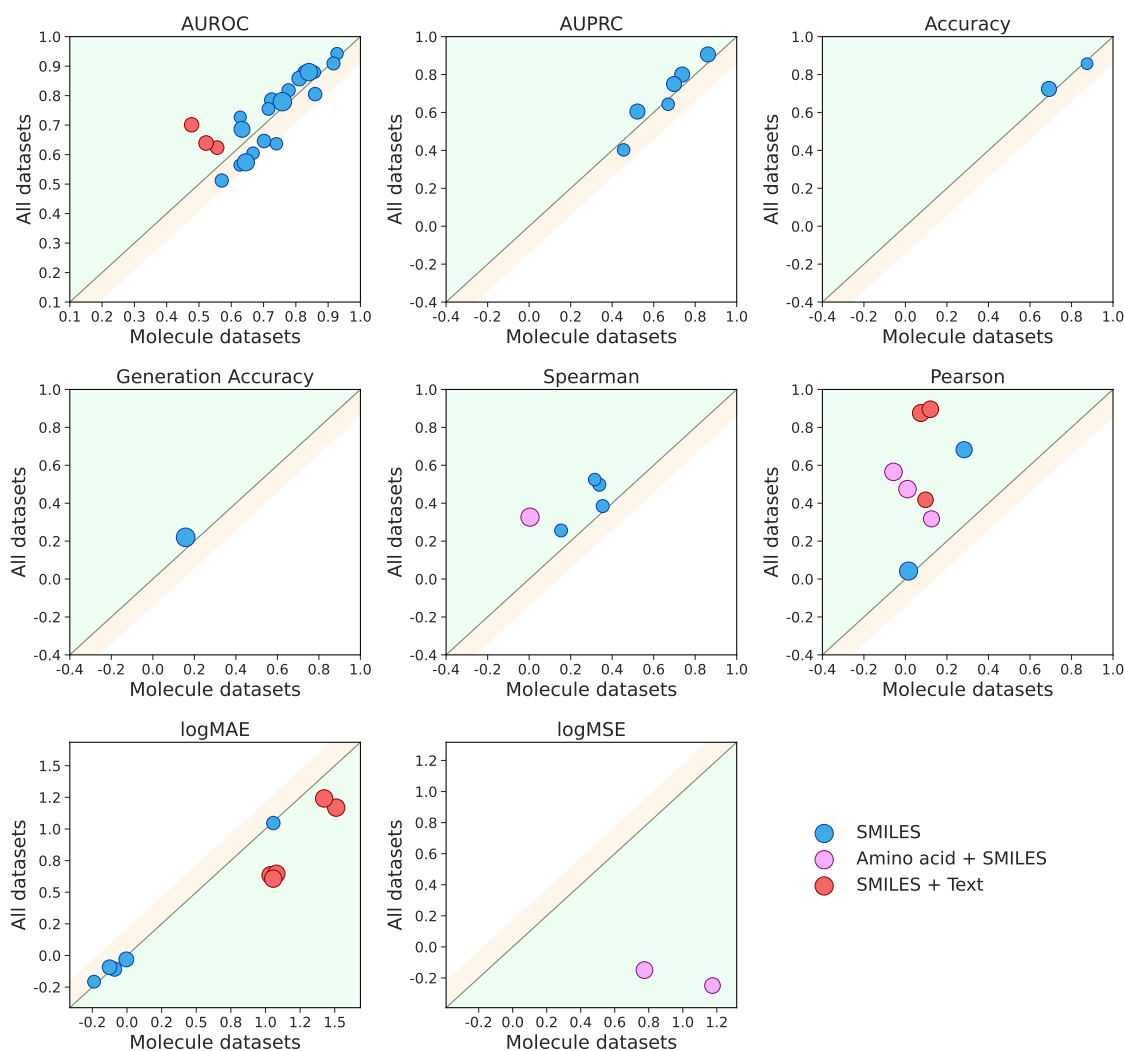


Figure 4 | Tx-LLM shows evidence of positive transfer across datasets with diverse drug types. Performance of Tx-LLM (S) finetuned and evaluated on small molecule datasets. “All datasets” indicates a Tx-LLM (S) model finetuned on all TDC datasets, and “Molecule datasets” indicates a Tx-LLM (S) model finetuned on datasets containing molecules (datasets involving other drug types such as proteins or nucleic acids are not included in training). Datasets are colored by their feature types indicated in the legend, and marker sizes illustrate the number of data points in the task on a log scale. The larger shaded area in green indicates where “All datasets” is better than “Molecule dataset” (showing evidence of positive transfer), while the narrower orange shaded area indicates where the performance of “Molecule datasets” is near the performance of “All dataset” (defined as within 10%). MAE and MSE values are log-transformed because the magnitudes of these values depend on the units of the outputs. Generation accuracy is the fraction of correct SMILES strings in the USPTO generation dataset.

differences in performance when evaluated on a single task [61].

Context removal We constructed a unique context for each TDC dataset that provides background information for Tx-LLM. We studied the effect of removing this context in Tables A.13 and A.14. We observed that removing the context reduced performance in 49 out of 66 datasets, which was also statistically significant ($\rho = 4.9 \times 10^{-6}$, Wilcoxon signed-rank test). Given that we trained a single set of weights for all TDC datasets, this suggests that providing context may be a useful way to allow generalist LLMs to become effective predictors for specific tasks. This was especially true for the ToxCast dataset, which contained numerous subtasks corresponding to predicting toxicity in various assays. Each ToxCast assay draws from the same set of small molecules and measures toxicity, but the toxicity label differs based on the particular assay used. Without providing assay-specific information in the context, the model would have no way of differentiating subtasks with different labels.

5 Discussion

To the best of our knowledge, Tx-LLM is the first LLM trained on a wide variety of TDC datasets including small molecules, proteins, nucleic acids, cells, and diseases all in a single model. Interestingly, we found that including datasets without small molecules in our training, such as those only using proteins, enhances performance on small molecule datasets compared to models trained only on small molecule datasets. A previous generalist AI model finetuned for the biomedical domain (Med-PaLM M [12]) observed positive transfer between chest X-ray report generation and chest X-ray classification tasks. There, the positive transfer was between tasks that were relatively closely related, as both tasks involved chest X-rays. However, the positive transfer observed in Tx-LLM is between molecular tasks using SMILES strings and protein tasks using amino acid sequences, which are quite different.

Although LLMs have demonstrated strong general language and reasoning capabilities, their effectiveness has been notably limited when it comes to tasks requiring specialized knowledge in chemistry [39, 68]. For example, it was found that InstructGPT [68] rarely produced invalid SMILES strings, possibly suggesting that SMILES strings were encountered during training, but InstructGPT was unable to correctly predict the molecule name from the SMILES string. Thus, while non-finetuned LLMs may be able to capture grammar, understanding deeper connections is difficult, and domain finetuning may be necessary to achieve strong performance for therapeutics.

LLMs have previously been challenged by mathematical problems and regression, as it has been observed that smaller models have underperformed on mathematical benchmarks, which may be related to lossy compression of numbers in the model hidden states [69]. However, Tx-LLM is often effective at performing regression, exceeding SOTA or achieving near-SOTA performance on 19 out of 29 regression datasets. In other work, Gruver *et al.* [8] found that LLMs could be used for time series prediction, which was attributed to the LLMs’ proclivity for periodicity often found in time series. LLMs have also been implemented as universal regressors [9], and LLMs finetuned for the chemistry domain have been used to perform regression tasks on molecules [41]. Taken together, these suggest that applying LLMs to regression problems may be a promising area to explore in multiple domains.

Since Tx-LLM is a generalist model trained on a wide variety of tasks, we propose that it can have a future role for end-to-end therapeutic development spanning early-stage development such as target discovery to late-stage development such as clinical trial approval. Figure 2 illustrates an example for the case of developing small molecule drugs against type 2 diabetes. Here, Tx-LLM can be effective at identifying genes associated with type 2 diabetes, predicting binding affinities of many small molecules against the protein target, predicting toxicities of the selected small molecules, and finally predicting the probability of clinical trial approval. Tx-LLM can also be used for other tasks that are not illustrated, such as predicting drug permeability and drug synthesis reactions.

However, at this stage, Tx-LLM is in the research stage with scope for further improvement as the model is not an effective predictor for every task. In particular, the integration of the Gemini family of models [70] with Tx-LLM remains an interesting possibility to enhance performance. Experimental validation and subsequent screening steps also remain an essential, complementary part of the therapeutic development pipeline. Overall, we believe the methodology behind Tx-LLM (including the creation of TxT and the development of fine-tuned

LLMs) represents a promising step towards using AI to contextualize and enhance many aspects of therapeutic development in future.

One important limitation of our work is that Tx-LLM is not instruction-tuned to follow natural language because we were primarily interested in the accuracy of its predictions and did not want to limit this ability by also constraining Tx-LLM to follow natural language. Therefore, unlike LLMs finetuned for medical question answering [10–12], Tx-LLM is unable to explain its predictions to the user. This limits the benefits gained by training over a wide variety of tasks and may be an interesting area for future work.

Additionally, it is important to note that LLMs are trained on large datasets, which increase the potential for data contamination and may result in overestimating their generalization. For Tx-LLM, our data contamination analysis suggests that there is little overlap between the PaLM-2 training data and our evaluation data, and filtering the overlapping datapoints does not result in decreased performance. Nonetheless, our analysis does not account for different formats between the PaLM-2 training data and TDC data (e.g. using molecule names vs SMILES strings), and prospectively analyzing the performance of Tx-LLM over time may be another avenue to study the effect of data contamination.

6 Conclusion

Therapeutic development is an expensive process that involves many potential types of therapeutics as well as many criteria for approval. AI models may be useful tools for reducing the failure rate of therapeutic development by providing initial screening for multiple aspects of the development pipeline. Although further development and validation is required, we believe Tx-LLM represents a notable advance towards a single generalist AI that can contextualize and aid many aspects of development ranging from target discovery to manufacturing.

Acknowledgments

This project was a collaboration between teams at Google Research and Google DeepMind. We thank David Belanger for the feedback and insight which significantly contributed to the enhancement of this report. We also thank Sami Lachgar, Lauren Winer, Maggie Shiels, Jessica Valdez, Jane Park, Jon Small, Aaron Abood, Rishad Patel, Uchechi Okereke, Annisah Um'rani, Alan Karthikesalingam, Anil Palepu, and Juraj Gottweis for their valuable insights, technical support and feedback during our research. We are also grateful to Zoubin Ghahramani, Raia Hadsell, Jon Shlens and Joelle Barral for their support during the course of this project.

Data availability

Datasets utilized for developing, benchmarking, and evaluation of Tx-LLM are publicly accessible with appropriate permissions. The Therapeutics Data Commons (TDC) datasets are accessible via their [website](#).

Competing interests

This study was funded by Alphabet Inc and/or a subsidiary thereof ('Alphabet'). T. T., C. S., D. F., V. N., and S. A. are employees of Alphabet and may own stock as part of the standard compensation package.

References

1. Sun, D., Gao, W., Hu, H. & Zhou, S. Why 90% of clinical drug development fails and how to improve it? en. *Acta Pharmaceutica Sinica B* **12**, 3049–3062. ISSN: 22113835. <https://linkinghub.elsevier.com/retrieve/pii/S2211383522000521> (2024) (July 2022).
2. Hinkson, I. V., Madej, B. & Stahlberg, E. A. Accelerating Therapeutics for Opportunities in Medicine: A Paradigm Shift in Drug Discovery. *Frontiers in Pharmacology* **11**, 770. ISSN: 1663-9812. <https://www.frontiersin.org/article/10.3389/fphar.2020.00770/full> (2024) (June 2020).
3. Lin, A., Giuliano, C. J., Palladino, A., John, K. M., Abramowicz, C., Yuan, M. L., Sausville, E. L., Lukow, D. A., Liu, L., Chait, A. R., Galluzzo, Z. C., Tucker, C. & Sheltzer, J. M. Off-target toxicity is a common mechanism of action of cancer drugs undergoing clinical trials. en. *Science Translational Medicine* **11**, eaaw8412. ISSN: 1946-6234, 1946-6242. <https://www.science.org/doi/10.1126/scitranslmed.aaw8412> (Sept. 2019).
4. Sadybekov, A. V. & Katritch, V. Computational approaches streamlining drug discovery. en. *Nature* **616**, 673–685. ISSN: 0028-0836, 1476-4687. <https://www.nature.com/articles/s41586-023-05905-z> (2024) (Apr. 2023).
5. Huang, K., Fu, T., Gao, W., Zhao, Y., Roohani, Y., Leskovec, J., Coley, C. W., Xiao, C., Sun, J. & Zitnik, M. Artificial intelligence foundation for therapeutic science. en. *Nature Chemical Biology* **18**, 1033–1036. ISSN: 1552-4450, 1552-4469. <https://www.nature.com/articles/s41589-022-01131-2> (2024) (Oct. 2022).
6. Huang, K., Fu, T., Gao, W., Zhao, Y., Roohani, Y., Leskovec, J., Coley, C. W., Xiao, C., Sun, J. & Zitnik, M. *Therapeutics Data Commons: Machine Learning Datasets and Tasks for Drug Discovery and Development* 2021. arXiv: 2102.09548 [cs.LG].
7. Robinson, J. & Wingate, D. *Leveraging Large Language Models for Multiple Choice Question Answering* in *The Eleventh International Conference on Learning Representations* (2023). <https://openreview.net/forum?id=yKbprarjc5B>.
8. Gruver, N., Finzi, M., Qiu, S. & Wilson, A. G. *Large Language Models Are Zero-Shot Time Series Forecasters* 2023. arXiv: 2310.07820 [cs.LG].
9. Song, X., Li, O., Lee, C., Yang, B., Peng, D., Perel, S. & Chen, Y. *OmniPred: Language Models as Universal Regressors* 2024. arXiv: 2402.14547 [cs.LG].
10. Singhal, K., Azizi, S., Tu, T., Mahdavi, S. S., Wei, J., Chung, H. W., Scales, N., Tanwani, A., Cole-Lewis, H., Pfohl, S., Payne, P., Seneviratne, M., Gamble, P., Kelly, C., Babiker, A., Schärl, N., Chowdhery, A., Mansfield, P., Demner-Fushman, D., Agüera Y Arcas, B., Webster, D., Corrado, G. S., Matias, Y., Chou, K., Gottweis, J., Tomasev, N., Liu, Y., Rajkomar, A., Barral, J., Semturs, C., Karthikesalingam, A. & Natarajan, V. Large language models encode clinical knowledge. en. *Nature* **620**, 172–180. ISSN: 0028-0836, 1476-4687. <https://www.nature.com/articles/s41586-023-06291-2> (2024) (Aug. 2023).
11. Singhal, K., Tu, T., Gottweis, J., Sayres, R., Wulczyn, E., Hou, L., Clark, K., Pfohl, S., Cole-Lewis, H., Neal, D., Schaeckermann, M., Wang, A., Amin, M., Lachgar, S., Mansfield, P., Prakash, S., Green, B., Dominowska, E., y Arcas, B. A., Tomasev, N., Liu, Y., Wong, R., Semturs, C., Mahdavi, S. S., Barral, J., Webster, D., Corrado, G. S., Matias, Y., Azizi, S., Karthikesalingam, A. & Natarajan, V. *Towards Expert-Level Medical Question Answering with Large Language Models* 2023. arXiv: 2305.09617 [cs.CL].
12. Tu, T., Azizi, S., Driess, D., Schaeckermann, M., Amin, M., Chang, P.-C., Carroll, A., Lau, C., Tanno, R., Ktena, I., Mustafa, B., Chowdhery, A., Liu, Y., Kornblith, S., Fleet, D., Mansfield, P., Prakash, S., Wong, R., Virmani, S., Semturs, C., Mahdavi, S. S., Green, B., Dominowska, E., y Arcas, B. A., Barral, J., Webster, D., Corrado, G. S., Matias, Y., Singhal, K., Florence, P., Karthikesalingam, A. & Natarajan, V. *Towards Generalist Biomedical AI* 2023. arXiv: 2307.14334 [cs.CL].
13. Zhang, W., Wang, Q., Kong, X., Xiong, J., Ni, S., Cao, D., Niu, B., Chen, M., Zhang, R., Wang, Y., Zhang, L., Li, X., Xiong, Z., Shi, Q., Huang, Z., Fu, Z. & Zheng, M. *Fine-tuning Large Language Models for Chemical Text Mining* preprint (Chemistry, Feb. 2024). <https://chemrxiv.org/engage/chemrxiv/article-details/65baa07b9138d2316124f224> (2024).
14. Jablonka, K. M., Schwaller, P., Ortega-Guerrero, A. & Smit, B. Leveraging large language models for predictive chemistry. en. *Nature Machine Intelligence* **6**, 161–169. ISSN: 2522-5839. <https://www.nature.com/articles/s42256-023-00788-1> (2024) (Feb. 2024).
15. Vaswani, A., Shazeer, N., Parmar, N., Uszkoreit, J., Jones, L., Gomez, A. N., Kaiser, L. & Polosukhin, I. *Attention Is All You Need* 2023. arXiv: 1706.03762 [cs.CL].
16. Brown, T., Mann, B., Ryder, N., Subbiah, M., Kaplan, J. D., Dhariwal, P., Neelakantan, A., Shyam, P., Sastry, G., Askell, A., Agarwal, S., Herbert-Voss, A., Krueger, G., Henighan, T., Child, R., Ramesh, A., Ziegler, D., Wu, J., Winter, C., Hesse, C., Chen, M., Sigler, E., Litwin, M., Gray, S., Chess, B., Clark, J., Berner, C., McCandlish, S., Radford, A., Sutskever, I. & Amodei, D. *Language Models are Few-Shot Learners* in *Advances in Neural Information Processing Systems* (eds Larochelle, H., Ranzato, M., Hadsell, R., Balcan, M. & Lin, H.) **33** (Curran Associates, Inc., 2020), 1877–1901. https://proceedings.neurips.cc/paper_files/paper/2020/file/1457c0d6bfc4967418bfb8ac142f64a-Paper.pdf.
17. Raffel, C., Shazeer, N., Roberts, A., Lee, K., Narang, S., Matena, M., Zhou, Y., Li, W. & Liu, P. J. Exploring the Limits of Transfer Learning with a Unified Text-to-Text Transformer. *Journal of Machine Learning Research* **21**, 1–67. <http://jmlr.org/papers/v21/20-074.html> (2020).
18. Torng, W. & Altman, R. B. Graph Convolutional Neural Networks for Predicting Drug-Target Interactions. en. *Journal of Chemical Information and Modeling* **59**, 4131–4149. ISSN: 1549-9596, 1549-960X. <https://pubs.acs.org/doi/10.1021/acs.jcim.9b00628> (2024) (Oct. 2019).
19. Stärk, H., Ganea, O., Pattanaik, L., Barzilay, R. & Jaakkola, T. *Equibind: Geometric deep learning for drug binding structure prediction* in *International conference on machine learning* (2022), 20503–20521.
20. Xiong, Z., Wang, D., Liu, X., Zhong, F., Wan, X., Li, X., Li, Z., Luo, X., Chen, K., Jiang, H. & Zheng, M. Pushing the Boundaries of Molecular Representation for Drug Discovery with the Graph Attention Mechanism. en. *Journal of Medicinal Chemistry* **63**, 8749–8760. ISSN: 0022-2623, 1520-4804. <https://pubs.acs.org/doi/10.1021/acs.jmedchem.9b00959> (2024) (Aug. 2020).
21. Heid, E. & Green, W. H. Machine Learning of Reaction Properties via Learned Representations of the Condensed Graph of Reaction. en. *Journal of Chemical Information and Modeling* **62**, 2101–2110. ISSN: 1549-9596, 1549-960X. <https://pubs.acs.org/doi/10.1021/acs.jcim.1c00975> (2024) (May 2022).
22. Yang, K., Swanson, K., Jin, W., Coley, C., Eiden, P., Gao, H., Guzman-Perez, A., Hopper, T., Kelley, B., Mathea, M., Palmer, A., Settels, V., Jaakkola, T., Jensen, K. & Barzilay, R. Analyzing Learned Molecular Representations for Property Prediction. en. *Journal of Chemical Information and Modeling* **59**, 3370–3388. ISSN: 1549-9596, 1549-960X. <https://pubs.acs.org/doi/10.1021/acs.jcim.9b00237> (2024) (Aug. 2019).

23. Morrone, J. A., Weber, J. K., Huynh, T., Luo, H. & Cornell, W. D. Combining Docking Pose Rank and Structure with Deep Learning Improves Protein–Ligand Binding Mode Prediction over a Baseline Docking Approach. *Journal of Chemical Information and Modeling* **60**. PMID: 32077698, 4170–4179. eprint: <https://doi.org/10.1021/acs.jcim.9b00927> (2020).
24. Mohr, B., Shmilovich, K., Kleinwächter, I. S., Schneider, D., Ferguson, A. L. & Bereau, T. Data-driven discovery of cardiopilin-selective small molecules by computational active learning. en. *Chemical Science* **13**, 4498–4511. ISSN: 2041-6520, 2041-6539. <http://xlink.rsc.org/?DOI=D2SC00116K> (2024) (2022).
25. Stokes, J. M., Yang, K., Swanson, K., Jin, W., Cubillos-Ruiz, A., Donghia, N. M., MacNair, C. R., French, S., Carfrae, L. A., Bloom-Ackermann, Z., Tran, V. M., Chiappino-Pepe, A., Badran, A. H., Andrews, I. W., Chory, E. J., Church, G. M., Brown, E. D., Jaakkola, T. S., Barzilay, R. & Collins, J. J. A Deep Learning Approach to Antibiotic Discovery. en. *Cell* **180**, 688–702.e13. ISSN: 00928674. <https://linkinghub.elsevier.com/retrieve/pii/S0092867420301021> (2024) (Feb. 2020).
26. Ran, B., Chen, L., Li, M., Han, Y. & Dai, Q. Drug-Drug Interactions Prediction Using Fingerprint Only. en. *Computational and Mathematical Methods in Medicine* **2022** (ed Wei, L.) 1–14. ISSN: 1748-6718, 1748-670X. <https://www.hindawi.com/journals/cmnm/2022/7818480/> (2024) (May 2022).
27. Tayyebi, A., Alshami, A. S., Rabiei, Z., Yu, X., Ismail, N., Talukder, M. J. & Power, J. Prediction of organic compound aqueous solubility using machine learning: a comparison study of descriptor-based and fingerprints-based models. en. *Journal of Cheminformatics* **15**, 99. ISSN: 1758-2946. <https://jcheminf.biomedcentral.com/articles/10.1186/s13321-023-00752-6> (2024) (Oct. 2023).
28. Belenahalli Shekarappa, S., Kandagalla, S. & Lee, J. Development of machine learning models based on molecular fingerprints for selection of small molecule inhibitors against JAK2 protein. en. *Journal of Computational Chemistry* **44**, 1493–1504. ISSN: 0192-8651, 1096-987X. <https://onlinelibrary.wiley.com/doi/10.1002/jcc.27103> (2024) (June 2023).
29. Louie, R. H. Y., Kaczorowski, K. J., Barton, J. P., Chakraborty, A. K. & McKay, M. R. Fitness landscape of the human immunodeficiency virus envelope protein that is targeted by antibodies. *Proceedings of the National Academy of Sciences* **115**, E564–E573. eprint: <https://www.pnas.org/doi/pdf/10.1073/pnas.1717765115>. <https://www.pnas.org/doi/abs/10.1073/pnas.1717765115> (2018).
30. Gfeller, D., Schmidt, J., Croce, G., Guillaume, P., Bobisse, S., Genolet, R., Queiroz, L., Cesbron, J., Racle, J. & Harari, A. Improved predictions of antigen presentation and TCR recognition with MixMHCpred2.2 and PRIME2.0 reveal potent SARS-CoV-2 CD8⁺ T-cell epitopes. en. *Cell Systems* **14**, 72–83.e5. ISSN: 24054712. <https://linkinghub.elsevier.com/retrieve/pii/S2405471222004707> (2024) (Jan. 2023).
31. Motmaen, A., Dauparas, J., Baek, M., Abedi, M. H., Baker, D. & Bradley, P. Peptide-binding specificity prediction using fine-tuned protein structure prediction networks. *Proceedings of the National Academy of Sciences* **120**, e2216697120. eprint: <https://www.pnas.org/doi/pdf/10.1073/pnas.2216697120>. <https://www.pnas.org/doi/abs/10.1073/pnas.2216697120> (2023).
32. Wang, Y., Liu, Y., Wang, S., Liu, Z., Gao, Y., Zhang, H. & Dong, L. ATTFold: RNA Secondary Structure Prediction With Pseudoknots Based on Attention Mechanism. *Frontiers in Genetics* **11**, 612086. ISSN: 1664-8021. <https://www.frontiersin.org/articles/10.3389/fgene.2020.612086/full> (2024) (Dec. 2020).
33. Jumper, J., Evans, R., Pritzel, A., Green, T., Figurnov, M., Ronneberger, O., Tunyasuvunakool, K., Bates, R., Židek, A., Potapenko, A., Bridgland, A., Meyer, C., Kohl, S. A. A., Ballard, A. J., Cowie, A., Romera-Paredes, B., Nikolov, S., Jain, R., Adler, J., Back, T., Petersen, S., Reiman, D., Clancy, E., Zielinski, M., Steinegger, M., Pacholska, M., Berghammer, T., Bodenstein, S., Silver, D., Vinyals, O., Senior, A. W., Kavukcuoglu, K., Kohli, P. & Hassabis, D. Highly accurate protein structure prediction with AlphaFold. en. *Nature* **596**, 583–589. ISSN: 0028-0836, 1476-4687. <https://www.nature.com/articles/s41586-021-03819-2> (2024) (Aug. 2021).
34. Tunyasuvunakool, K., Adler, J., Wu, Z., Green, T., Zielinski, M., Židek, A., Bridgland, A., Cowie, A., Meyer, C., Laydon, A., Velankar, S., Kleywegt, G. J., Bateman, A., Evans, R., Pritzel, A., Figurnov, M., Ronneberger, O., Bates, R., Kohl, S. A. A., Potapenko, A., Ballard, A. J., Romera-Paredes, B., Nikolov, S., Jain, R., Clancy, E., Reiman, D., Petersen, S., Senior, A. W., Kavukcuoglu, K., Birney, E., Kohli, P., Jumper, J. & Hassabis, D. Highly accurate protein structure prediction for the human proteome. en. *Nature* **596**, 590–596. ISSN: 0028-0836, 1476-4687. <https://www.nature.com/articles/s41586-021-03828-1> (2024) (Aug. 2021).
35. Senior, A. W., Evans, R., Jumper, J., Kirkpatrick, J., Sifre, L., Green, T., Qin, C., Židek, A., Nelson, A. W. R., Bridgland, A., Penedones, H., Petersen, S., Simonyan, K., Crossan, S., Kohli, P., Jones, D. T., Silver, D., Kavukcuoglu, K. & Hassabis, D. Improved protein structure prediction using potentials from deep learning. en. *Nature* **577**, 706–710. ISSN: 0028-0836, 1476-4687. <https://www.nature.com/articles/s41586-019-1923-7> (2024) (Jan. 2020).
36. Abramson, J., Adler, J., Dunger, J., Evans, R., Green, T., Pritzel, A., Ronneberger, O., Willmore, L., Ballard, A. J., Bambrick, J., Bodenstein, S. W., Evans, D. A., Hung, C.-C., O'Neill, M., Reiman, D., Tunyasuvunakool, K., Wu, Z., Žemgulytė, A., Arvaniti, E., Beattie, C., Bertolli, O., Bridgland, A., Cherepanov, A., Congreve, M., Cowen-Rivers, A. I., Cowie, A., Figurnov, M., Fuchs, F. B., Gladman, H., Jain, R., Khan, Y. A., Low, C. M. R., Perlin, K., Potapenko, A., Savy, P., Singh, S., Stecula, A., Thillaisundaram, A., Tong, C., Yakneen, S., Zhong, E. D., Zielinski, M., Židek, A., Bapst, V., Kohli, P., Jaderberg, M., Hassabis, D. & Jumper, J. M. Accurate structure prediction of biomolecular interactions with AlphaFold 3. en. *Nature*. ISSN: 0028-0836, 1476-4687. <https://www.nature.com/articles/s41586-024-07487-w> (2024) (May 2024).
37. Ren, F., Ding, X., Zheng, M., Korzinkin, M., Cai, X., Zhu, W., Mantsyzov, A., Aliper, A., Aladinskiy, V., Cao, Z., Kong, S., Long, X., Man Liu, B. H., Liu, Y., Naumov, V., Shneyderman, A., Ozerov, I. V., Wang, J., Pun, F. W., Polykovskiy, D. A., Sun, C., Levitt, M., Aspuru-Guzik, A. & Zhavoronkov, A. AlphaFold accelerates artificial intelligence powered drug discovery: efficient discovery of a novel CDK20 small molecule inhibitor. en. *Chemical Science* **14**, 1443–1452. ISSN: 2041-6520, 2041-6539. <https://xlink.rsc.org/?DOI=D2SC05709C> (2024) (2023).
38. Higgins, M. K. Can We AlphaFold Our Way Out of the Next Pandemic? en. *Journal of Molecular Biology* **433**, 167093. ISSN: 00222836. <https://linkinghub.elsevier.com/retrieve/pii/S002228362100317X> (2024) (Oct. 2021).
39. White, A. D., Hocky, G. M., Gandhi, H. A., Ansari, M., Cox, S., Wellawatte, G. P., Sasmal, S., Yang, Z., Liu, K., Singh, Y. & Peña Ccoa, W. J. Assessment of chemistry knowledge in large language models that generate code. *Digital Discovery* **2**, 368–376. <http://dx.doi.org/10.1039/D2DD00087C> (2 2023).
40. Guo, T., Guo, K., Nan, B., Liang, Z., Guo, Z., Chawla, N. V., Wiest, O. & Zhang, X. What can Large Language Models do in chemistry? A comprehensive benchmark on eight tasks in Thirty-seventh Conference on Neural Information Processing Systems Datasets and Benchmarks Track (2023). <https://openreview.net/forum?id=IngBR3SZHW>.

41. Yu, B., Baker, F. N., Chen, Z., Ning, X. & Sun, H. *LlaSMol: Advancing Large Language Models for Chemistry with a Large-Scale, Comprehensive, High-Quality Instruction Tuning Dataset* 2024. arXiv: 2402.09391 [cs.AI].
42. M. Bran, A., Cox, S., Schilter, O., Baldassari, C., White, A. D. & Schwaller, P. Augmenting large language models with chemistry tools. en. *Nature Machine Intelligence*. ISSN: 2522-5839. <https://www.nature.com/articles/s42256-024-00832-8> (2024) (May 2024).
43. Rives, A., Meier, J., Sercu, T., Goyal, S., Lin, Z., Liu, J., Guo, D., Ott, M., Zitnick, C. L., Ma, J. & Fergus, R. Biological Structure and Function Emerge from Scaling Unsupervised Learning to 250 Million Protein Sequences. *PNAS*. <https://www.biorxiv.org/content/10.1101/622803v4> (2019).
44. Lin, Z., Akin, H., Rao, R., Hie, B., Zhu, Z., Lu, W., Smetanin, N., Verkuil, R., Kabeli, O., Shmueli, Y., Dos Santos Costa, A., Fazel-Zarandi, M., Sercu, T., Candido, S. & Rives, A. Evolutionary-scale prediction of atomic-level protein structure with a language model. en. *Science* **379**, 1123–1130. ISSN: 0036-8075, 1095-9203. <https://www.science.org/doi/10.1126/science.ade2574> (2024) (Mar. 2023).
45. Alley, E. C., Khimulya, G., Biswas, S., AlQuraishi, M. & Church, G. M. Unified rational protein engineering with sequence-based deep representation learning. en. *Nature Methods* **16**, 1315–1322. ISSN: 1548-7091, 1548-7105. <https://www.nature.com/articles/s41592-019-0598-1> (2024) (Dec. 2019).
46. Ferruz, N., Schmidt, S. & Höcker, B. ProtGPT2 is a deep unsupervised language model for protein design. en. *Nature Communications* **13**, 4348. ISSN: 2041-1723. <https://www.nature.com/articles/s41467-022-32007-7> (2024) (July 2022).
47. Hie, B., Zhong, E. D., Berger, B. & Bryson, B. Learning the language of viral evolution and escape. *Science* **371**, 284–288. eprint: <https://www.science.org/doi/pdf/10.1126/science.abd7331>. <https://www.science.org/doi/abs/10.1126/science.abd7331> (2021).
48. Hie, B. L., Shanker, V. R., Xu, D., Bruun, T. U. J., Weidenbacher, P. A., Tang, S., Wu, W., Pak, J. E. & Kim, P. S. Efficient evolution of human antibodies from general protein language models. en. *Nature Biotechnology* **42**, 275–283. ISSN: 1087-0156, 1546-1696. <https://www.nature.com/articles/s41587-023-01763-2> (2024) (Feb. 2024).
49. Zhuo, L., Chi, Z., Xu, M., Huang, H., Zheng, H., He, C., Mao, X.-L. & Zhang, W. *ProtLLM: An Interleaved Protein-Language LLM with Protein-as-Word Pre-Training* 2024. arXiv: 2403.07920 [q-bio.BM].
50. Pei, Q., Zhang, W., Zhu, J., Wu, K., Gao, K., Wu, L., Xia, Y. & Yan, R. *BioT5: Enriching Cross-modal Integration in Biology with Chemical Knowledge and Natural Language Associations* 2024. arXiv: 2310.07276 [cs.CL].
51. Cui, H., Wang, C., Maan, H., Pang, K., Luo, F., Duan, N. & Wang, B. scGPT: toward building a foundation model for single-cell multi-omics using generative AI. en. *Nature Methods*. ISSN: 1548-7091, 1548-7105. <https://www.nature.com/articles/s41592-024-02201-0> (2024) (Feb. 2024).
52. Chen, Y. & Zou, J. GenePT: A Simple But Effective Foundation Model for Genes and Cells Built From ChatGPT. *bioRxiv*. eprint: <https://www.biorxiv.org/content/early/2024/03/05/2023.10.16.562533.full.pdf> (2024).
53. Theodoris, C. V., Xiao, L., Chopra, A., Chaffin, M. D., Al Sayed, Z. R., Hill, M. C., Mantineo, H., Brydon, E. M., Zeng, Z., Liu, X. S. & Ellinor, P. T. Transfer learning enables predictions in network biology. en. *Nature* **618**, 616–624. ISSN: 0028-0836, 1476-4687. <https://www.nature.com/articles/s41586-023-06139-9> (2024) (June 2023).
54. Kim, S., Chen, J., Cheng, T., Gindulyte, A., He, J., He, S., Li, Q., Shoemaker, B. A., Thiessen, P. A., Yu, B., *et al.* PubChem 2023 update. *Nucleic acids research* **51**, D1373–D1380 (2023).
55. ToxCast and Tox21 Summary Files from invitrodb_v3. <https://www.epa.gov/chemical-research/toxicity-forecaster-toxcasttm-data> (2015).
56. Lowe, D. Chemical reactions from US patents (1976-Sep2016). https://figshare.com/articles/dataset/Chemical_reactions_from_US_patents_1976-Sep2016_/5104873 (June 2017).
57. Nielsen, M. & Andreatta, M. NetMHCpan-3.0; improved prediction of binding to MHC class I molecules integrating information from multiple receptor and peptide length datasets. en. *Genome Medicine* **8**, 33. ISSN: 1756-994X. <https://genomemedicine.biomedcentral.com/articles/10.1186/s13073-016-0288-x> (2024) (Dec. 2016).
58. Jensen, K. K., Andreatta, M., Marcatili, P., Buus, S., Greenbaum, J. A., Yan, Z., Sette, A., Peters, B. & Nielsen, M. Improved methods for predicting peptide binding affinity to MHC class II molecules. en. *Immunology* **154**, 394–406. ISSN: 0019-2805, 1365-2567. <https://onlinelibrary.wiley.com/doi/10.1111/imm.12889> (2024) (July 2018).
59. Google *et al.* *PaLM 2 Technical Report* 2023. arXiv: 2305.10403 [cs.CL].
60. Barham, P., Chowdhery, A., Dean, J., Ghemawat, S., Hand, S., Hurt, D., Isard, M., Lim, H., Pang, R., Roy, S., Saeta, B., Schuh, P., Sepassi, R., Shafey, L. E., Thekkath, C. A. & Wu, Y. *Pathways: Asynchronous Distributed Dataflow for ML* 2022. arXiv: 2203.12533 [cs.DC].
61. Longpre, S., Hou, L., Vu, T., Webson, A., Chung, H. W., Tay, Y., Zhou, D., Le, Q. V., Zoph, B., Wei, J. & Roberts, A. *The Flan Collection: Designing Data and Methods for Effective Instruction Tuning* 2023. arXiv: 2301.13688 [cs.AI].
62. Landrum, G. RDKit: Open-Source Cheminformatics Software. https://github.com/rdkit/rdkit/releases/tag/Release_2016_09_4 (2016).
63. Dalke, A. The chemfp project. en. *Journal of Cheminformatics* **11**, 76. ISSN: 1758-2946. <https://jcheminf.biomedcentral.com/articles/10.1186/s13321-019-0398-8> (2024) (Dec. 2019).
64. Sievers, F., Wilm, A., Dineen, D., Gibson, T. J., Karplus, K., Li, W., Lopez, R., McWilliam, H., Remmert, M., Söding, J., Thompson, J. D. & Higgins, D. G. Fast, scalable generation of high-quality protein multiple sequence alignments using Clustal Omega. en. *Molecular Systems Biology* **7**, 539. ISSN: 1744-4292, 1744-4292. <https://www.embopress.org/doi/10.1038/msb.2011.75> (2024) (Jan. 2011).
65. Fu, T., Huang, K., Xiao, C., Glass, L. M. & Sun, J. HINT: Hierarchical interaction network for clinical-trial-outcome predictions. *Patterns* **3**, 100445. ISSN: 2666-3899. <https://www.sciencedirect.com/science/article/pii/S2666389922000186> (2022).
66. Wigh, D. S., Goodman, J. M. & Lapkin, A. A. A review of molecular representation in the age of machine learning. *WIREs Computational Molecular Science* **12**, e1603. eprint: <https://wires.onlinelibrary.wiley.com/doi/pdf/10.1002/wcms.1603>. <https://wires.onlinelibrary.wiley.com/doi/abs/10.1002/wcms.1603> (2022).
67. Kinnings, S. L., Liu, N., Tonge, P. J., Jackson, R. M., Xie, L. & Bourne, P. E. A Machine Learning-Based Method To Improve Docking Scoring Functions and Its Application to Drug Repurposing. en. *Journal of Chemical Information and Modeling* **51**, 408–419. ISSN: 1549-9596, 1549-960X. <https://pubs.acs.org/doi/10.1021/ci100369f> (2024) (Feb. 2011).

68. Ouyang, L., Wu, J., Jiang, X., Almeida, D., Wainwright, C. L., Mishkin, P., Zhang, C., Agarwal, S., Slama, K., Ray, A., Schulman, J., Hilton, J., Kelton, F., Miller, L., Simens, M., Aspell, A., Welinder, P., Christiano, P., Leike, J. & Lowe, R. *Training language models to follow instructions with human feedback* 2022. arXiv: 2203.02155 [[cs.CL](#)].
69. Zhu, F., Dai, D. & Sui, Z. *Language Models Understand Numbers, at Least Partially* 2024. arXiv: 2401.03735 [[cs.CL](#)].
70. Team, G. *et al. Gemini: A Family of Highly Capable Multimodal Models* 2024. arXiv: 2312.11805 [[cs.CL](#)].

Appendix

A.1 Additional data details

Table A.1 | Excluded TDC datasets and reasons for exclusion.

Dataset name	Reason for exclusion
QM7b	Prediction of quantum properties is not closely related to therapeutic development.
QM8	Prediction of quantum properties is not closely related to therapeutic development.
QM9	Prediction of quantum properties is not closely related to therapeutic development.
IEDB Jespersen	Amount of data is small, and token prediction is more difficult to implement in a LLM than binary classification.
PDB Jespersen	Amount of data is small, and token prediction is more difficult to implement in a LLM than binary classification.
DrugBank DDI	Large number of possible labels is difficult to implement in a LLM.
TWOSIDES	Large number of possible labels is difficult to implement in a LLM.
USPTO Catalyst	Large number of possible labels is difficult to implement in a LLM.
MOSES	No clear metric.
ZINC	No clear metric.
ChEMBL	No clear metric.
USPTO 50K	Subset of USPTO.
USPTO Reaction	Same dataset as USPTO.

Table A.2 | Hyperparameters used for Tx-LLM finetuning.

Hyperparameter	Tx-LLM (S)	Tx-LLM (M)
Learning rate	3×10^{-5}	1×10^{-4}
Dropout rate	0.05	0.15
Batch size	256	256
Max token input length	2048	2048
Max token output length	512	512

Table A.3 | Example of prompts for binary classification datasets.

Instructions: Answer the following question about drug properties.

Context: As a membrane separating circulating blood and brain extracellular fluid, the blood-brain barrier (BBB) is the protection layer that blocks most foreign drugs. Thus the ability of a drug to penetrate the barrier to deliver to the site of action forms a crucial challenge in development of drugs for central nervous system.

Question: Given a drug SMILES string, predict whether it

(A) does not cross the BBB (B) crosses the BBB

Drug SMILES: CN1C(=O)CN=C(C2=CCCC2)c2cc(Cl)ccc21

Answer: (B)

Instructions: Answer the following question about peptide-MHC binding.

Context: In the human body, T cells monitor the existing peptides and trigger an immune response if the peptide is foreign. To decide whether or not if the peptide is not foreign, the peptide must bind to a major histocompatibility complex (MHC) molecule. Therefore, predicting peptide-MHC binding affinity is pivotal for determining immunogenicity. In some experiments, the peptide binding is measured against cells that express multiple MHCs, so the peptide could be binding any one of the possible MHCs. Class 1 MHC molecules bind to peptides that are usually 8-14 amino acids long and activate CD8 T cells.

Question: Given the amino acid sequence of the peptide and possible pseudo amino acid sequences of MHC 1, predict whether the peptide

(A) does not bind to any of the MHCs (B) binds to any of the MHCs

Peptide amino acid sequence: QLADETLLKV

Possible MHC pseudosequences: YFAMYGEKVAHTHVDTLYVRYHYTTWAEWAYTWY

Answer: (B)

Instructions: Answer the following question about miRNA protein interactions.

Context: MicroRNAs (miRNAs) are, small non-coding RNAs with 18–25 nucleotides, which are central regulators at the post-transcriptional level in both animals and plants. Perfect or near-perfect complementary binding of miRNAs and their target mRNA negatively regulates gene expression by accelerating mRNA degradation or suppressing mRNA translation.

Question: Given the miRNA mature sequence and target amino acid sequence, predict whether

(A) the miRNA and target do not interact (B) the miRNA and target interact

miRNA sequence: UUCCUGUCAGCCGUGGGUGCC

Target amino acid sequence: MSVNMDLRHQVMINQFVLAAGCAADQAKQLLQAAHWQFETALSTFF QETNIPNSHHHHQMMCTPSNTPATPPNFPDALAMFSKLRASEGLQSSNSPMTAAACSP-PANFSPFWASSPPSHQAPWIPSSPTTFHHLHRPQPTWPPGAQQGGAQQKAMAAMDGQR

Answer: (A)

Instructions: Answer the following question about clinical trials.

Context: Clinical trial is the most time and cost-consuming step in the drug discovery process. Phase 1 clinical trials test the safety and basic properties of a new drug or treatment in a small group of people for the first time. Optimizing and designing trials with machine learning could drastically lead to the speedup of delivery of life-saving therapeutics to patients. Clinical trial outcome prediction is a machine learning task that aims to forecast the outcome of clinical trials, such as the approval rate of a drug or treatment. It utilizes various clinical trial features, including the drug’s molecular structure and patient disease.

Question: Given a drug SMILES string and disease, predict if the phase 1 trial

(A) would not be approved (B) would be approved

Drug SMILES: COC1=NC(N)=NC2=C1N=CN2[C@@H]1O[C@H](CO)[C@@H](O)[C@@H]1O

Disease: Chronic myeloproliferative disease

Answer: (A)

Table A.4 | Example of prompts for regression and generation datasets.

Instructions: Answer the following question about drug properties.

Context: The human colon epithelial cancer cell line, Caco-2, is used as an in vitro model to simulate the human intestinal tissue. The experimental result on the rate of drug passing through the Caco-2 cells can approximate the rate at which the drug permeates through the human intestinal tissue.

Question: Given a drug SMILES string, predict its normalized Caco-2 cell effective permeability from 000 to 1000, where 000 is minimum permeability and 1000 is maximum permeability.

Drug SMILES: O=C(O)COC(=O)Cc1ccccc1Nc1c(Cl)cccc1Cl

Answer: 788

Instructions: Answer the following question about drug responses.

Context: The same drug compound could have various levels of responses in different patients. To design drug for individual or a group with certain characteristics is the central goal of precision medicine. In experiments, IC50s of drugs were measured against cancer cell lines.

Question: Given a drug SMILES string and a cell line description, predict the normalized drug sensitivity from 000 to 1000, where 000 is minimum drug sensitivity and 1000 is maximum drug sensitivity.

Drug SMILES: CN1C=C(C2=CC=CC=C21)/C=C\3/C4=C(C=CC=N4)NC3=O

Cell line description: SNU-1, stomach cell sourced from cancer

Answer: 615

Instructions: Answer the following question about drug target interactions.

Context: Drug-target binding is the physical interaction between a drug and a specific biological molecule, such as a protein or enzyme. This interaction is essential for the drug to exert its pharmacological effect. The strength of the drug-target binding is determined by the binding affinity, which is a measure of how tightly the drug binds to the target. Kd is the dissociation constant of a drug-target complex. It is the concentration of drug at which half of the drug-target complexes have dissociated. A lower Kd value indicates a stronger binding affinity.

Question: Given the target amino acid sequence and compound SMILES string, predict their normalized binding affinity Kd from 000 to 1000, where 000 is minimum Kd and 1000 is maximum Kd.

Drug SMILES: O=S(=O)(O)c1cccc2cccc(Nc3ccccc3)c12

Target amino acid sequence: MATVQQLEGRWRLVDSKGFDEYMKELGVGIALRKMGMAMAKPDC IITCDGKNLTIKTESTLKTTFQFCTLGEEKFEETTADGRKTQTVCFNFTD GALVQH QHEWDGK- ESTITRKLKDGKLVVECVMMNVTCTRIYEKVE

Answer: 397

Instructions: Answer the following question about reactions.

Context: Retrosynthesis is the process of finding a set of reactants that can synthesize a target molecule, i.e., product, which is a fundamental task in drug manufacturing. The target is recursively transformed into simpler precursor molecules until commercially available "starting" molecules are identified. In a data sample, there is only one product molecule, reactants can be one or multiple molecules.

Question: Given a product SMILES string, predict the reactant SMILES string.

Product SMILES: [CH2:12]1[C:7]2([CH2:6][CH2:5][O:15][CH2:1][CH2:8]2)[CH2:13][CH2:14][O:10][C:11]1=[O:17]

Answer: [CH:1]12B[CH:5]([CH2:6][CH2:7][CH2:8]1)CCC2.[O:10]1[CH2:14][CH2:13][CH2:12][CH2:11]1.[OH:-:15].[Na+].[OH:17]O.Cl

Table A.5 | Example of a 10-shot prompt for a binary classification dataset.

Instructions: Answer the following question about drug properties.

Context: As a membrane separating circulating blood and brain extracellular fluid, the blood-brain barrier (BBB) is the protection layer that blocks most foreign drugs. Thus the ability of a drug to penetrate the barrier to deliver to the site of action forms a crucial challenge in development of drugs for central nervous system.

Question: Given a drug SMILES string, predict whether it
(A) does not cross the BBB (B) crosses the BBB

Drug SMILES: CN1C(=O)CN=C(c2ccccc2)c2cc(Cl)ccc21

Answer: (B)

Drug SMILES: CN1C(=O)CN=C(c2ccccc2F)c2cc(Cl)ccc21

Answer: (B)

Drug SMILES: CN1C(=S)CN=C(c2ccccc2)c2cc(Cl)ccc21

Answer: (B)

Drug SMILES: CP(C)(=O)CN1C(=O)CN=C(c2ccccc2)c2cc(Cl)ccc21

Answer: (B)

Drug SMILES: CN1C(=O)CN=C(c2ccccc2)c2cc([N+](=O)[O-])ccc21

Answer: (B)

Drug SMILES: CCN(CC)CCN1C(=O)CN=C(c2ccccc2F)c2cc(Cl)ccc21

Answer: (B)

Drug SMILES: O=C1CN=C(c2ccccc2)c2cc(Cl)ccc2N1CC1CC1

Answer: (B)

Drug SMILES: C#CCN1C(=O)CN=C(c2ccccc2)c2cc(Cl)ccc21

Answer: (B)

Drug SMILES: O=C1CN=C(c2ccccc2)c2cc(Cl)ccc2N1CC(F)(F)F

Answer: (B)

Drug SMILES: CCS(=O)(=O)CCN1C(=O)CN=C(c2ccccc2F)c2cc(Cl)ccc21

Answer: (B)

Drug SMILES: CN1C(=O)CN=C(C2=CCCCC2)c2cc(Cl)ccc21

Answer: (B)

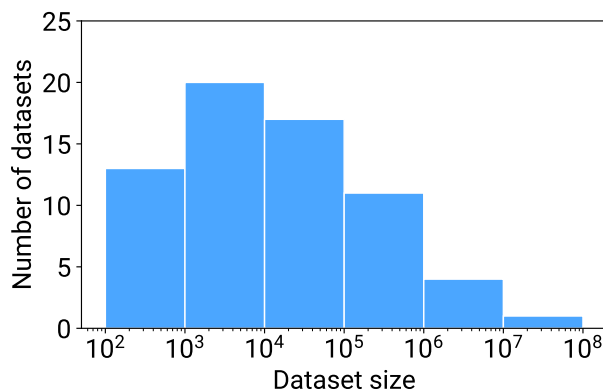


Figure A.1 | Distribution of TDC dataset sizes, aggregated over train, validation, and test sets. For datasets containing multiple subtasks, such as ToxCast which contains data for more than 600 different assays, the dataset size is calculated by summing over the sizes for each subtask.

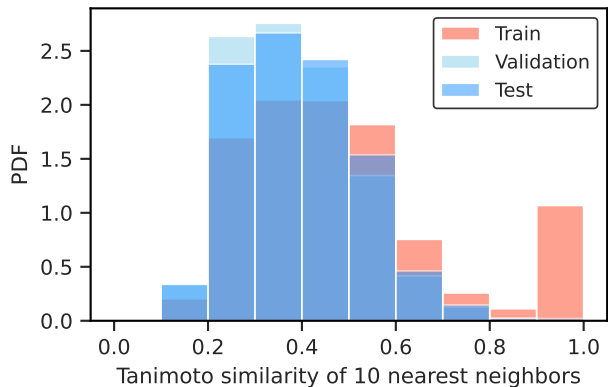


Figure A.2 | Distribution of the Tanimoto similarities for the 10 nearest neighbors in the AMES dataset. Nearest neighbors are calculated from the training set for training and validation sets, and from both the training and validation sets for the test set.

A.2 Additional results

Table A.6 | Median relative difference of Tx-LLM (M) performance from SOTA for datasets grouped by feature type. The relative difference is defined as $(\text{Tx-LLM performance} - \text{SOTA}) / \text{SOTA}$. The signs were reversed for MAE and MSE metrics because lower MAE and MSE values correspond to better performances.

Feature type	Median relative difference of Tx-LLM performance from SOTA
SMILES + Text	0.048
Nucleotide + Amino acid	-0.007
Amino acid	-0.080
SMILES	-0.082
Amino acid + SMILES	-0.482
Nucleotide	-0.888

Table A.7 | Tx-LLM (M) performance compared with SOTA for each binary classification dataset, along with the feature types and metric type. Performances that are better than SOTA are bolded.

Dataset name	Feature type	Split method	Metric	SOTA	Tx-LLM
PAMPA NCATS	SMILES	Scaffold	AUROC	0.900 [1]	0.668
HIA Hou	SMILES	Scaffold	AUROC	0.988 [2]	0.990
Pgp Broccatelli	SMILES	Scaffold	AUROC	0.935 [3]	0.939
Bioavailability Ma	SMILES	Scaffold	AUROC	0.748 [4]	0.702
BBB Martins	SMILES	Scaffold	AUROC	0.915 [5]	0.882
CYP2C19 Veith	SMILES	Scaffold	AUROC	0.890 [6]	0.895
CYP2D6 Veith	SMILES	Scaffold	AUPRC	0.739 [7]	0.659
CYP3A4 Veith	SMILES	Scaffold	AUPRC	0.904 [7]	0.840
CYP1A2 Veith	SMILES	Scaffold	AUPRC	0.900 [8]	0.914
CYP2C9 Veith	SMILES	Scaffold	AUPRC	0.839 [7]	0.788
CYP2C9 Substrate CarbonMangels	SMILES	Scaffold	AUPRC	0.441 [9]	0.436
CYP2D6 Substrate CarbonMangels	SMILES	Scaffold	AUPRC	0.736 [7]	0.600
CYP3A4 Substrate CarbonMangels	SMILES	Scaffold	AUROC	0.662 [10]	0.647
hERG	SMILES	Scaffold	AUROC	0.874 [4]	0.909
AMES	SMILES	Scaffold	AUROC	0.871 [3]	0.786
DILI	SMILES	Scaffold	AUROC	0.925 [3]	0.882
Skin Reaction	SMILES	Scaffold	AUROC	0.840 [11]	0.615
Carcinogens Lagunin	SMILES	Scaffold	Accuracy	0.770 [12]	0.786
Tox21	SMILES	Scaffold	AUROC	0.961 [13]	0.882
ClinTox	SMILES	Scaffold	AUROC	0.948 [14]	0.863
herg central	SMILES	Scaffold	AUROC	0.860 [15]	0.888
hERG Karim	SMILES	Scaffold	Accuracy	0.770 [16]	0.745
ToxCast	SMILES	Scaffold	AUROC	0.777 [14]	0.792
SARSCoV2 Vitro Touret	SMILES	Scaffold	AUROC	0.640 [17]	0.601
SARSCOV2 3CLPro Diamond	SMILES	Scaffold	AUROC	0.800 [18]	0.712
HIV	SMILES	Scaffold	AUROC	0.851 [19]	0.732
SAbDab Chen	Amino acid	Random	AUPRC	0.510 [20]	0.473
HuRI	Amino acid	Cold-start	AUPRC	0.724 [21]	0.753
miRTarBase	Nucleotide + Amino acid	Random	Accuracy	0.804 [22]	0.799
MHC1 IEDB IMGT Nielsen	Amino acid	Random	AUROC	0.986 [23]	0.907
MHC2 IEDB Jensen	Amino acid	Random	AUROC	0.940 [24]	0.863
weber	Amino acid	Cold-start	AUROC	0.870 [25]	0.743
phase1	SMILES + Text	Cold-start	AUROC	0.576 [26]	0.667
phase2	SMILES + Text	Cold-start	AUROC	0.645 [26]	0.676
phase3	SMILES + Text	Cold-start	AUROC	0.723 [26]	0.728
butkiewicz	SMILES	Random	AUROC	0.840 [27]	0.566

Table A.8 | Tx-LLM (M) performance compared with SOTA for each regression and generation dataset, along with the feature types and metric type. Performances that are better than SOTA are bolded. Datasets for which we did not find a SOTA are marked as N/A.

Dataset name	Feature type	Split method	Metric	SOTA	Tx-LLM
Caco2 Wang	SMILES	Scaffold	MAE	0.285 [2]	0.432
Lipophilicity AstraZeneca	SMILES	Scaffold	MAE	0.467 [28]	0.587
Solubility AqSolDB	SMILES	Scaffold	MAE	0.761 [28]	0.987
PPBR AZ	SMILES	Scaffold	MAE	7.788 [28]	9.108
VDss Lombardo	SMILES	Scaffold	Spearman	0.627 [29]	0.609
Half Life Obach	SMILES	Scaffold	Spearman	0.547 [30]	0.448
Clearance Hepatocyte AZ	SMILES	Scaffold	Spearman	0.440 [31]	0.385
Clearance Microsome AZ	SMILES	Scaffold	Spearman	0.625 [2]	0.413
LD50 Zhu	SMILES	Scaffold	MAE	0.552 [32]	0.618
USPTO Yields	SMILES	Random	Pearson	0.361 [33]	0.070
Buchwald Hartwig	SMILES	Random	Pearson	0.786 [33]	0.905
TAP	Amino acid	Random	MAE	N/A	4.983
Leenay	Nucleotide	Random	Spearman	0.740 [34]	0.083
BindingDB kd	Amino acid + SMILES	Cold-start	Pearson	0.712 [35]	0.391
BindingDB ic50	Amino acid + SMILES	Cold-start	Spearman	0.637 [36]	0.311
BindingDB ki	Amino acid + SMILES	Cold-start	Pearson	0.840 [37]	0.726
BindingDB Patent	Amino acid + SMILES	Temporal	Pearson	0.588 [38]	0.531
DAVIS	Amino acid + SMILES	Cold-start	MSE	0.219 [39]	0.704
KIBA	Amino acid + SMILES	Cold-start	MSE	0.154 [39]	0.548
DisGeNET	Amino acid + Text	Random	MAE	N/A	0.057
GDSC1	SMILES + Text	Random	Pearson	0.860 [40]	0.887
GDSC2	SMILES + Text	Random	Pearson	0.860 [40]	0.900
DrugComb CSS	SMILES + Text	Combination	MAE	16.858 [41]	14.057
OncoPolyPharmacology	SMILES + Text	Combination	Pearson	0.730 [42]	0.552
Protein SAbDab	Amino acid	Random	MAE	N/A	1.268
DrugComb HSA	SMILES + Text	Combination	MAE	4.453 [41]	4.118
DrugComb Loewe	SMILES + Text	Combination	MAE	9.184 [41]	17.381
DrugComb Bliss	SMILES + Text	Combination	MAE	4.560 [41]	4.104
DrugComb ZIP	SMILES + Text	Combination	MAE	4.027 [41]	3.777
USPTO	SMILES	Random	Generation Accuracy	0.415 [43]	0.239

Table A.9 | Performances on binary classification datasets for PaLM 2 (S), PaLM 2 (M), Tx-LLM (S) and Tx-LLM (M). The best performances are bolded.

Dataset name	Metric	PaLM 2 (S)	PaLM 2 (M)	Tx-LLM (S)	Tx-LLM (M)
PAMPA NCATS	AUROC	0.640	0.661	0.646	0.668
HIA Hou	AUROC	0.837	0.711	0.942	0.990
Pgp Broccatelli	AUROC	0.791	0.848	0.909	0.939
Bioavailability Ma	AUROC	0.492	0.564	0.605	0.702
BBB Martins	AUROC	0.732	0.616	0.805	0.882
CYP2C19 Veith	AUROC	0.608	0.627	0.877	0.895
CYP2D6 Veith	AUPRC	0.170	0.198	0.605	0.659
CYP3A4 Veith	AUPRC	0.544	0.544	0.800	0.840
CYP1A2 Veith	AUPRC	0.590	0.594	0.906	0.914
CYP2C9 Veith	AUPRC	0.336	0.401	0.750	0.788
CYP2C9 Substrate CarbonMangels	AUPRC	0.340	0.308	0.403	0.436
CYP2D6 Substrate CarbonMangels	AUPRC	0.380	0.575	0.643	0.600
CYP3A4 Substrate CarbonMangels	AUROC	0.560	0.604	0.637	0.647
hERG	AUROC	0.701	0.756	0.879	0.909
AMES	AUROC	0.614	0.563	0.785	0.786
DILI	AUROC	0.643	0.741	0.727	0.882
Skin Reaction	AUROC	0.431	0.553	0.564	0.615
Carcinogens Lagunin	Accuracy	0.821	0.714	0.857	0.786
Tox21	AUROC	0.406	0.610	0.858	0.882
ClinTox	AUROC	0.387	0.471	0.818	0.863
herg central	AUROC	0.491	0.509	0.880	0.888
hERG Karim	Accuracy	0.570	0.555	0.724	0.745
ToxCast	AUROC	0.455	0.530	0.779	0.792
SARSCoV2 Vitro Touret	AUROC	0.580	0.556	0.512	0.601
SARSCOV2 3CLPro Diamond	AUROC	0.371	0.619	0.755	0.712
HIV	AUROC	0.436	0.494	0.686	0.732
SAbDab Chen	AUPRC	0.437	0.545	0.390	0.473
HuRI	AUPRC	0.509	0.501	0.705	0.753
miRTarBase	Accuracy	0.502	0.499	0.765	0.799
MHC1 IEDB IMGT Nielsen	AUROC	0.548	0.557	0.913	0.907
MHC2 IEDB Jensen	AUROC	0.617	0.604	0.781	0.863
weber	AUROC	0.666	0.680	0.738	0.743
phase1	AUROC	0.524	0.490	0.624	0.667
phase2	AUROC	0.529	0.519	0.639	0.676
phase3	AUROC	0.527	0.508	0.701	0.728
butkiewicz	AUROC	0.504	0.499	0.574	0.566

Table A.10 | Performances on regression and generation datasets for PaLM 2 (S), PaLM 2 (M), Tx-LLM (S) and Tx-LLM (M). The best performances are bolded.

Dataset name	Metric	PaLM 2 (S)	PaLM 2 (M)	Tx-LLM (S)	Tx-LLM (M)
Caco2 Wang	MAE	0.457	1.680	0.621	0.432
Lipophilicity AstraZeneca	MAE	1.108	1.189	0.779	0.587
Solubility AqSolDB	MAE	2.536	5.427	0.931	0.987
PPBR AZ	MAE	13.104	32.447	11.138	9.108
VDss Lombardo	Spearman	-0.062	0.174	0.497	0.609
Half Life Obach	Spearman	-0.033	0.380	0.525	0.448
Clearance Hepatocyte AZ	Spearman	0.240	0.075	0.256	0.385
Clearance Microsome AZ	Spearman	0.337	0.024	0.385	0.413
LD50 Zhu	MAE	0.823	0.971	0.808	0.618
USPTO Yields	Pearson	0.001	0.002	0.042	0.070
Buchwald Hartwig	Pearson	0.333	0.089	0.682	0.905
TAP	MAE	2.480	3.536	5.075	4.983
Leenay	Spearman	0.004	-0.010	0.048	0.083
BindingDB kd	Pearson	0.089	0.087	0.317	0.391
BindingDB ic50	Spearman	0.033	-0.114	0.326	0.311
BindingDB ki	Pearson	0.055	0.026	0.565	0.726
BindingDB Patent	Pearson	-0.022	0.031	0.474	0.531
DAVIS	MSE	5.102	5.145	0.564	0.704
KIBA	MSE	8.530	8.777	0.709	0.548
DisGeNET	MAE	0.088	0.134	0.059	0.057
GDSC1	Pearson	-0.042	0.006	0.876	0.887
GDSC2	Pearson	-0.058	0.010	0.896	0.900
DrugComb CSS	MAE	27.159	24.66	14.740	14.057
OncoPolyPharmacology	Pearson	0.056	0.017	0.418	0.552
Protein SAbDab	MAE	1.282	1.236	1.432	1.268
DrugComb HSA	MAE	5.885	4.485	4.311	4.118
DrugComb Loewe	MAE	16.456	20.865	17.428	17.381
DrugComb Bliss	MAE	5.675	4.565	4.425	4.104
DrugComb ZIP	MAE	5.735	4.742	4.047	3.777
USPTO	Generation Accuracy	0.000	0.000	0.220	0.239

Table A.11 | Performances on binary classification datasets for varying few-shot prompting strategies with Tx-LLM (S). The number of shots is varied between 0, 1, 5, and 10, and the shots are either chosen randomly or based on the nearest neighbors (KNN). Nearest neighbors are determined by Tanimoto similarities for molecules and sequence identity for proteins and nucleotides. The best performances are bolded.

Dataset name	Metric	0-shot	1-shot random	5-shot random	10-shot random	1-shot KNN	5-shot KNN	10-shot KNN
PAMPA NCATS	AUROC	0.677	0.650	0.649	0.633	0.671	0.662	0.646
HIA Hou	AUROC	0.956	0.960	0.947	0.939	0.953	0.952	0.942
Pgp Broccatelli	AUROC	0.906	0.903	0.908	0.908	0.905	0.908	0.909
Bioavailability Ma	AUROC	0.607	0.616	0.619	0.597	0.611	0.606	0.605
BBB Martins	AUROC	0.807	0.806	0.800	0.799	0.811	0.808	0.805
CYP2C19 Veith	AUROC	0.874	0.875	0.876	0.875	0.875	0.877	0.877
CYP2D6 Veith	AUPRC	0.598	0.600	0.601	0.604	0.604	0.605	0.605
CYP3A4 Veith	AUPRC	0.801	0.802	0.802	0.799	0.803	0.803	0.800
CYP1A2 Veith	AUPRC	0.906	0.907	0.906	0.906	0.907	0.906	0.906
CYP2C9 Veith	AUPRC	0.751	0.748	0.752	0.750	0.748	0.751	0.750
CYP2C9 Substrate CarbonMangels	AUPRC	0.416	0.408	0.423	0.411	0.412	0.414	0.403
CYP2D6 Substrate CarbonMangels	AUPRC	0.624	0.634	0.624	0.624	0.637	0.648	0.643
CYP3A4 Substrate CarbonMangels	AUROC	0.645	0.645	0.640	0.639	0.646	0.641	0.637
hERG	AUROC	0.869	0.868	0.868	0.877	0.873	0.875	0.879
AMES	AUROC	0.780	0.784	0.781	0.783	0.781	0.783	0.785
DILI	AUROC	0.697	0.708	0.702	0.715	0.717	0.713	0.727
Skin Reaction	AUROC	0.572	0.566	0.544	0.549	0.570	0.552	0.564
Carcinogens Lagumin	Accuracy	0.839	0.857	0.875	0.893	0.857	0.857	0.857
Tox21	AUROC	0.857	0.856	0.858	0.856	0.858	0.858	0.858
ClinTox	AUROC	0.801	0.796	0.800	0.814	0.811	0.807	0.818
herg central	AUROC	0.878	0.879	0.880	0.880	0.880	0.879	0.880
hERG Karim	Accuracy	0.711	0.709	0.714	0.715	0.714	0.725	0.724
ToxCast	AUROC	0.777	0.778	0.778	0.777	0.779	0.779	0.779
SARSCoV2 Vitro Touret	AUROC	0.525	0.526	0.519	0.542	0.521	0.525	0.512
SARSCOV2 3CLPro Diamond	AUROC	0.723	0.739	0.744	0.748	0.717	0.746	0.755
HIV	AUROC	0.675	0.683	0.691	0.686	0.675	0.686	0.686
SAbDab Chen	AUPRC	0.369	0.390	0.385	0.373	0.399	0.385	0.390
HuRI	AUPRC	0.698	0.705	0.705	0.705	0.705	0.705	0.705
miRTarBase	Accuracy	0.765	0.765	0.765	0.765	0.765	0.765	0.765
MHC1 IEDB IMGT Nielsen	AUROC	0.912	0.913	0.913	0.913	0.913	0.913	0.913
MHC2 IEDB Jensen	AUROC	0.775	0.780	0.780	0.783	0.778	0.778	0.781
weber	AUROC	0.737	0.738	0.738	0.738	0.738	0.738	0.738
phase1	AUROC	0.628	0.634	0.627	0.628	0.631	0.628	0.624
phase2	AUROC	0.641	0.642	0.640	0.638	0.642	0.640	0.639
phase3	AUROC	0.693	0.696	0.697	0.692	0.695	0.697	0.701
butkiewicz	AUROC	0.581	0.548	0.582	0.593	0.558	0.538	0.574

Table A.12 | Performances on regression and generation datasets for varying few-shot prompting strategies with Tx-LLM (S). The number of shots is varied between 0, 1, 5, and 10, and the shots are either chosen randomly or based on the nearest neighbors (KNN). Nearest neighbors are determined by Tanimoto similarities for molecules and sequence identity for proteins and nucleotides. The best performances are bolded.

Dataset name	Metric	0-shot	1-shot random	5-shot random	10-shot random	1-shot KNN	5-shot KNN	10-shot KNN
Caco2 Wang	MAE	0.605	0.621	0.627	0.613	0.616	0.597	0.621
Lipophilicity AstraZeneca	MAE	0.803	0.812	0.791	0.782	0.818	0.793	0.779
Solubility AqSolDB	MAE	0.899	0.918	0.915	0.921	0.919	0.917	0.931
PPBR AZ	MAE	10.814	10.727	10.854	11.024	10.935	11.129	11.138
VDss Lombardo	Spearman	0.496	0.496	0.508	0.487	0.486	0.488	0.497
Half Life Obach	Spearman	0.494	0.502	0.503	0.489	0.523	0.499	0.525
Clearance Hepatocyte AZ	Spearman	0.255	0.285	0.252	0.258	0.285	0.303	0.256
Clearance Microsome AZ	Spearman	0.401	0.406	0.401	0.406	0.403	0.386	0.385
LD50 Zhu	MAE	0.815	0.811	0.809	0.809	0.810	0.807	0.808
USPTO Yields	Pearson	0.010	0.044	0.040	0.038	0.044	0.042	0.042
Buchwald Hartwig	Pearson	0.736	0.802	0.809	0.491	0.800	0.808	0.682
TAP	MAE	5.150	5.092	5.137	5.029	5.087	5.075	5.075
Leenay	Spearman	0.036	0.035	0.034	0.063	0.032	0.055	0.048
BindingDB kd	Pearson	0.314	0.314	0.320	0.305	0.320	0.318	0.317
BindingDB ic50	Spearman	0.331	0.327	0.327	0.327	0.327	0.326	0.326
BindingDB ki	Pearson	0.569	0.574	0.568	0.568	0.576	0.565	0.565
BindingDB Patent	Pearson	0.483	0.474	0.474	0.474	0.474	0.474	0.474
DAVIS	MSE	0.561	0.561	0.570	0.561	0.561	0.564	0.564
KIBA	MSE	0.743	0.711	0.715	0.718	0.707	0.709	0.709
DisGeNET	MAE	0.060	0.059	0.059	0.059	0.059	0.059	0.059
GDSC1	Pearson	0.876	0.876	0.875	0.875	0.876	0.876	0.876
GDSC2	Pearson	0.895	0.895	0.895	0.895	0.895	0.895	0.896
DrugComb CSS	MAE	14.779	14.775	14.729	14.749	14.781	14.743	14.740
OncoPolyPharmacology	Pearson	0.423	0.427	0.427	0.418	0.432	0.424	0.418
Protein SAbDab	MAE	1.399	1.384	1.427	1.406	1.398	1.420	1.432
DrugComb HSA	MAE	4.298	4.297	4.300	4.312	4.296	4.299	4.311
DrugComb Loewe	MAE	17.425	17.454	17.435	17.424	17.455	17.440	17.428
DrugComb Bliss	MAE	4.284	4.284	4.293	4.352	4.285	4.294	4.425
DrugComb ZIP	MAE	4.014	4.021	4.035	4.045	4.022	4.035	4.047
USPTO	Generation Accuracy	0.225	0.221	0.212	0.209	0.221	0.220	0.220

Table A.13 | Performances on binary classification datasets with Tx-LLM (S) using 10-shot KNN prompting, with and without context. The best performances are bolded.

Dataset name	Metric	10-shot KNN no context	10-shot KNN with context
PAMPA NCATS	AUROC	0.664	0.646
HIA Hou	AUROC	0.905	0.942
Pgp Broccatelli	AUROC	0.884	0.909
Bioavailability Ma	AUROC	0.592	0.605
BBB Martins	AUROC	0.797	0.805
CYP2C19 Veith	AUROC	0.875	0.877
CYP2D6 Veith	AUPRC	0.596	0.605
CYP3A4 Veith	AUPRC	0.805	0.800
CYP1A2 Veith	AUPRC	0.898	0.906
CYP2C9 Veith	AUPRC	0.750	0.750
CYP2C9 Substrate CarbonMangels	AUPRC	0.358	0.403
CYP2D6 Substrate CarbonMangels	AUPRC	0.645	0.643
CYP3A4 Substrate CarbonMangels	AUROC	0.639	0.637
hERG	AUROC	0.868	0.879
AMES	AUROC	0.747	0.785
DILI	AUROC	0.633	0.727
Skin Reaction	AUROC	0.529	0.564
Carcinogens Lagunin	Accuracy	0.857	0.857
Tox21	AUROC	0.828	0.858
ClinTox	AUROC	0.759	0.818
herg central	AUROC	0.876	0.880
hERG Karim	Accuracy	0.728	0.724
ToxCast	AUROC	0.719	0.779
SARSCoV2 Vitro Touret	AUROC	0.550	0.512
SARSCOV2 3CLPro Diamond	AUROC	0.765	0.755
HIV	AUROC	0.668	0.686
SAbDab Chen	AUPRC	0.415	0.390
HuRI	AUPRC	0.703	0.705
miRTarBase	Accuracy	0.765	0.765
MHC1 IEDB IMGT Nielsen	AUROC	0.912	0.913
MHC2 IEDB Jensen	AUROC	0.786	0.781
weber	AUROC	0.738	0.738
phase1	AUROC	0.608	0.624
phase2	AUROC	0.635	0.639
phase3	AUROC	0.691	0.701
butkiewicz	AUROC	0.621	0.574

Table A.14 | Performances on regression and generation datasets with Tx-LLM (S) using 10-shot KNN prompting, with and without context. The best performances are bolded.

Dataset name	Metric	10-shot KNN no context	10-shot KNN with context
Caco2 Wang	MAE	0.713	0.621
Lipophilicity AstraZeneca	MAE	0.765	0.779
Solubility AqSolDB	MAE	1.101	0.931
PPBR AZ	MAE	34.763	11.138
VDss Lombardo	Spearman	0.489	0.497
Half Life Obach	Spearman	0.389	0.525
Clearance Hepatocyte AZ	Spearman	0.219	0.256
Clearance Microsome AZ	Spearman	0.401	0.385
LD50 Zhu	MAE	0.818	0.808
USPTO Yields	Pearson	0.041	0.042
Buchwald Hartwig	Pearson	0.655	0.682
TAP	MAE	5.711	5.075
Leenay	Spearman	0.036	0.048
BindingDB kd	Pearson	0.309	0.317
BindingDB ic50	Spearman	0.318	0.326
BindingDB ki	Pearson	0.547	0.565
BindingDB Patent	Pearson	0.466	0.474
DAVIS	MSE	0.564	0.564
KIBA	MSE	0.704	0.709
DisGeNET	MAE	0.060	0.059
GDSC1	Pearson	0.875	0.876
GDSC2	Pearson	0.818	0.896
DrugComb CSS	MAE	21.656	14.740
OncoPolyPharmacology	Pearson	0.380	0.418
Protein SAbDab	MAE	1.433	1.432
DrugComb HSA	MAE	4.374	4.311
DrugComb Loewe	MAE	18.923	17.428
DrugComb Bliss	MAE	4.843	4.425
DrugComb ZIP	MAE	5.315	4.047
USPTO	Generation Accuracy	0.221	0.220

Table A.15 | Performance of Tx-LLM (S) finetuned on different datasets and evaluated with 10-shot KNN prompting on binary classification datasets. "All datasets" indicates a Tx-LLM (S) model finetuned on all TDC datasets, "molecule datasets" indicates a Tx-LLM (S) model finetuned on datasets containing molecules (datasets only involving other drug types such as proteins or nucleic acids are not included in training), and "ADMET datasets" indicates a Tx-LLM (S) model finetuned on datasets in the ADMET benchmark, which only contains molecules.

Dataset name	Feature type	In ADMET	Metric	All datasets	Molecule datasets	ADMET datasets
HIA Hou	SMILES	Yes	AUROC	0.942	0.928	0.915
Pgp Broccatelli	SMILES	Yes	AUROC	0.909	0.917	0.852
Bioavailability Ma	SMILES	Yes	AUROC	0.605	0.667	0.713
BBB Martins	SMILES	Yes	AUROC	0.805	0.860	0.843
CYP2D6 Veith	SMILES	Yes	AUPRC	0.605	0.522	0.418
CYP3A4 Veith	SMILES	Yes	AUPRC	0.800	0.737	0.736
CYP2C9 Veith	SMILES	Yes	AUPRC	0.750	0.698	0.609
CYP2C9 Substrate CarbonMangels	SMILES	Yes	AUPRC	0.403	0.455	0.328
CYP2D6 Substrate CarbonMangels	SMILES	Yes	AUPRC	0.643	0.670	0.683
CYP3A4 Substrate CarbonMangels	SMILES	Yes	AUROC	0.637	0.740	0.683
hERG	SMILES	Yes	AUROC	0.879	0.857	0.753
AMES	SMILES	Yes	AUROC	0.785	0.726	0.672
DILI	SMILES	Yes	AUROC	0.727	0.628	0.524
phase1	SMILES + Text	No	AUROC	0.624	0.556	0.534
phase2	SMILES + Text	No	AUROC	0.639	0.522	0.503
phase3	SMILES + Text	No	AUROC	0.701	0.477	0.492
PAMPA NCATS	SMILES	No	AUROC	0.646	0.702	0.717
CYP2C19 Veith	SMILES	No	AUROC	0.877	0.829	0.797
CYP1A2 Veith	SMILES	No	AUPRC	0.906	0.861	0.607
Skin Reaction	SMILES	No	AUROC	0.564	0.627	0.388
Carcinogens Lagunin	SMILES	No	Accuracy	0.857	0.875	0.714
Tox21	SMILES	No	AUROC	0.858	0.811	0.662
ClinTox	SMILES	No	AUROC	0.818	0.778	0.411
herg central	SMILES	No	AUROC	0.880	0.840	0.663
hERG Karim	SMILES	No	Accuracy	0.724	0.691	0.654
ToxCast	SMILES	No	AUROC	0.779	0.758	0.632
SARSCoV2 Vitro Touret	SMILES	No	AUROC	0.512	0.571	0.570
SARSCOV2 3CLPro Diamond	SMILES	No	AUROC	0.755	0.715	0.690
HIV	SMILES	No	AUROC	0.686	0.633	0.421
butkiewicz	SMILES	No	AUROC	0.574	0.645	0.498
miRTarBase	Nucleotide + Amino acid	No	Accuracy	0.765	0.499	0.502
SAbDab Chen	Amino acid	No	AUPRC	0.390	0.694	0.735
HuRI	Amino acid	No	AUPRC	0.705	0.513	0.513
MHC1 IEDB IMGT Nielsen	Amino acid	No	AUROC	0.913	0.675	0.650
MHC2 IEDB Jensen	Amino acid	No	AUROC	0.781	0.718	0.714
weber	Amino acid	No	AUROC	0.738	0.689	0.688

Table A.16 | Performance of Tx-LLM (S) finetuned on different datasets and evaluated with 10-shot KNN prompting on regression and generation datasets. "All datasets" indicates a Tx-LLM (S) model finetuned on all TDC datasets, "molecule datasets" indicates a Tx-LLM (S) model finetuned on datasets containing molecules (datasets only involving other drug types such as proteins or nucleic acids are not included in training), and "ADMET datasets" indicates a Tx-LLM (S) model finetuned on datasets in the ADMET benchmark, which only contains molecules.

Dataset name	Feature type	In ADMET	Metric	All datasets	Molecule datasets	ADMET datasets
Caco2 Wang	SMILES	Yes	MAE	0.621	0.578	0.555
Lipophilicity AstraZeneca	SMILES	Yes	MAE	0.779	0.815	0.813
Solubility AqSolDB	SMILES	Yes	MAE	0.931	0.989	0.929
PPBR AZ	SMILES	Yes	MAE	11.138	11.394	11.441
VDss Lombardo	SMILES	Yes	Spearman	0.497	0.338	0.412
Half Life Obach	SMILES	Yes	Spearman	0.525	0.316	0.267
Clearance Hepatocyte AZ	SMILES	Yes	Spearman	0.256	0.154	0.262
Clearance Microsome AZ	SMILES	Yes	Spearman	0.385	0.354	0.519
LD50 Zhu	SMILES	Yes	MAE	0.808	0.749	0.713
GDSC1	SMILES + Text	No	Pearson	0.876	0.075	0.146
GDSC2	SMILES + Text	No	Pearson	0.896	0.120	0.135
DrugComb CSS	SMILES + Text	No	MAE	14.740	32.394	26.871
OncoPolyPharmacology	SMILES + Text	No	Pearson	0.418	0.097	0.159
DrugComb HSA	SMILES + Text	No	MAE	4.311	10.883	5.127
DrugComb Loewe	SMILES + Text	No	MAE	17.428	26.516	12.242
DrugComb Bliss	SMILES + Text	No	MAE	4.425	11.984	5.603
DrugComb ZIP	SMILES + Text	No	MAE	4.047	11.367	5.351
USPTO Yields	SMILES	No	Pearson	0.042	0.015	0.007
Buchwald Hartwig	SMILES	No	Pearson	0.682	0.283	0.554
USPTO	SMILES	No	Generation Accuracy	0.220	0.158	0.000
Leenay	Nucleotide	No	Spearman	0.048	-0.006	-0.014
DisGeNET	Amino acid + Text	No	MAE	0.059	0.511	0.432
BindingDB kd	Amino acid + SMILES	No	Pearson	0.317	0.126	-0.001
BindingDB ic50	Amino acid + SMILES	No	Spearman	0.326	0.004	0.156
BindingDB ki	Amino acid + SMILES	No	Pearson	0.565	-0.057	-0.049
BindingDB Patent	Amino acid + SMILES	No	Pearson	0.474	0.010	-0.030
DAVIS	Amino acid + SMILES	No	MSE	0.564	14.955	5.631
KIBA	Amino acid + SMILES	No	MSE	0.709	5.950	3.391
TAP	Amino acid	No	MAE	5.075	6.491	5.024
Protein SAbDab	Amino acid	No	MAE	1.432	1.864	1.067

Table A.17 | The percent of each dataset’s test set containing features that also exist in the PaLM-2 training data, excluding datasets with no overlap at all.

Dataset name	Percent overlap with PaLM-2 training data	Metric	Unfiltered performance	Filtered performance
TAP	10.42	MAE	4.983	4.560
HuRI	5.93	AUPRC	0.753	0.756
SAbDab Chen	5.39	AUPRC	0.473	0.529
phase3	0.28	AUROC	0.723	0.727
BindingDB kd	0.09	Pearson	0.391	0.391
miRTarBase	0.04	Accuracy	0.804	0.799
DisGeNET	0.02	MAE	0.057	0.057

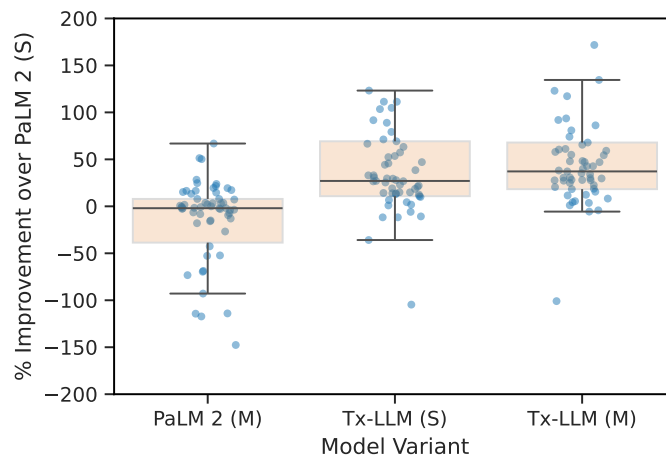


Figure A.3 | The percent improvement of PaLM 2 (M), Tx-LLM (S), and Tx-LLM (M) compared to PaLM 2 (S) for all TDC tasks.

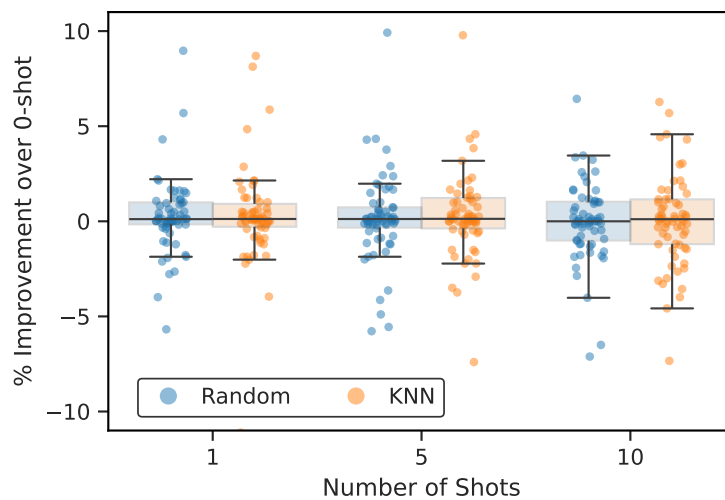


Figure A.4 | The percent improvement of few-shot prompting over 0-shot prompting with Tx-LLM (S). The number of shots and the shot selection method (random or KNN) are varied.

References

1. Siramshetty, V., Williams, J., Nguyen, Đ.-T., Neyra, J., Southall, N., Mathé, E., Xu, X. & Shah, P. Validating ADME QSAR Models Using Marketed Drugs. *SLAS DISCOVERY: Advancing the Science of Drug Discovery* **26**. PMID: 34176369, 1326–1336. eprint: <https://doi.org/10.1177/24725552211017520>. <https://doi.org/10.1177/24725552211017520> (2021).
2. Li, A. & Huang, D. *ADMET property prediction with Oloren ChemEngine* 2022.
3. Turon, G., Hlozek, J., Woodland, J. G., Kumar, A., Chibale, K. & Duran-Frigola, M. First fully-automated AI/ML virtual screening cascade implemented at a drug discovery centre in Africa. en. *Nature Communications* **14**, 5736. ISSN: 2041-1723. <https://www.nature.com/articles/s41467-023-41512-2> (2024) (Sept. 2023).
4. Bera, S., Dent, J., Gill, G., Stolman, A. & Wu, B. *SimGCN for TDC Benchmarks* 2022.
5. Fontenot, R., Kathad, U., McDermott, J., Sturtevant, D., Sharma, P. & Carr, P. *Predicting a Compounds Blood-Brain-Barrier Permeability with Lantern Pharma's AI and ML Platform, RADR* 2023.
6. Plonka, W., Stork, C., Šícho, M. & Kirchmair, J. CYPlebrity: Machine learning models for the prediction of inhibitors of cytochrome P450 enzymes. en. *Bioorganic & Medicinal Chemistry* **46**, 116388. ISSN: 09680896. <https://linkinghub.elsevier.com/retrieve/pii/S0968089621003965> (2024) (Sept. 2021).
7. Hu, W., Liu, B., Gomes, J., Zitnik, M., Liang, P., Pande, V. S. & Leskovec, J. Pre-training Graph Neural Networks. *CoRR abs/1905.12265*. arXiv: 1905.12265. <http://arxiv.org/abs/1905.12265> (2019).
8. Plonka, W., Stork, C., Šícho, M. & Kirchmair, J. CYPlebrity: Machine learning models for the prediction of inhibitors of cytochrome P450 enzymes. en. *Bioorganic & Medicinal Chemistry* **46**, 116388. ISSN: 09680896. <https://linkinghub.elsevier.com/retrieve/pii/S0968089621003965> (2024) (Sept. 2021).
9. Turon, G., Hlozek, J., Woodland, J. G., Kumar, A., Chibale, K. & Duran-Frigola, M. First fully-automated AI/ML virtual screening cascade implemented at a drug discovery centre in Africa. en. *Nature Communications* **14**, 5736. ISSN: 2041-1723. <https://www.nature.com/articles/s41467-023-41512-2> (2024) (Sept. 2023).
10. Huang, K., Fu, T., Glass, L. M., Zitnik, M., Xiao, C. & Sun, J. DeepPurpose: a deep learning library for drug–target interaction prediction. *Bioinformatics* **36**, 5545–5547. ISSN: 1367-4803. eprint: <https://academic.oup.com/bioinformatics/article-pdf/36/22-23/5545/50716143/btaa1005.pdf>. <https://doi.org/10.1093/bioinformatics/btaa1005> (Dec. 2020).
11. Alves, V. M., Muratov, E., Fourches, D., Strickland, J., Kleinstreuer, N., Andrade, C. H. & Tropsha, A. Predicting chemically-induced skin reactions. Part I: QSAR models of skin sensitization and their application to identify potentially hazardous compounds. *Toxicology and Applied Pharmacology* **284**, 262–272. ISSN: 0041-008X. <https://www.sciencedirect.com/science/article/pii/S0041008X14004529> (2015).
12. Lagunin, A., Filimonov, D., Zakharov, A., Xie, W., Huang, Y., Zhu, F., Shen, T., Yao, J. & Poroikov, V. Computer-Aided Prediction of Rodent Carcinogenicity by PASS and CISOC-PSCT. *QSAR & Combinatorial Science* **28**, 806–810. eprint: <https://onlinelibrary.wiley.com/doi/pdf/10.1002/qsar.200860192>. <https://onlinelibrary.wiley.com/doi/abs/10.1002/qsar.200860192> (2009).
13. Shermukhamedov, S., Mamurjonova, D. & Probst, M. *Structure to Property: Chemical Element Embeddings and a Deep Learning Approach for Accurate Prediction of Chemical Properties* 2023. arXiv: 2309.09355 [physics.chem-ph].
14. Li, P., Li, Y., Hsieh, C.-Y., Zhang, S., Liu, X., Liu, H., Song, S. & Yao, X. TrimNet: learning molecular representation from triplet messages for biomedicine. *Briefings in Bioinformatics* **22**, bbaa266. ISSN: 1477-4054. eprint: <https://academic.oup.com/bib/article-pdf/22/4/bbaa266/39144778/bbaa266.pdf>. <https://doi.org/10.1093/bib/bbaa266> (Nov. 2020).
15. Korotcov, A., Tkachenko, V., Russo, D. P. & Ekins, S. Comparison of Deep Learning With Multiple Machine Learning Methods and Metrics Using Diverse Drug Discovery Data Sets. en. *Molecular Pharmacology* **14**, 4462–4475. ISSN: 1543-8384, 1543-8392. <https://pubs.acs.org/doi/10.1021/acs.molpharmaceut.7b00578> (2024) (Dec. 2017).
16. Karim, A., Lee, M., Balle, T. & Sattar, A. CardioTox net: a robust predictor for hERG channel blockade based on deep learning meta-feature ensembles. en. *Journal of Cheminformatics* **13**, 60. ISSN: 1758-2946. <https://jcheminf.biomedcentral.com/articles/10.1186/s13321-021-00541-z> (2024) (Dec. 2021).
17. Liu, Y., Wu, Y., Shen, X. & Xie, L. COVID-19 Multi-Targeted Drug Repurposing Using Few-Shot Learning. *Frontiers in Bioinformatics* **1**, 693177. ISSN: 2673-7647. <https://www.frontiersin.org/articles/10.3389/fbinf.2021.693177/full> (2024) (June 2021).
18. Haneczok, J. & Delijewski, M. Machine learning enabled identification of potential SARS-CoV-2 3CLpro inhibitors based on fixed molecular fingerprints and Graph-CNN neural representations. *Journal of Biomedical Informatics* **119**, 103821. ISSN: 1532-0464. <https://www.sciencedirect.com/science/article/pii/S1532046421001507> (2021).
19. Li, J., Cai, D. & He, X. Learning Graph-Level Representation for Drug Discovery (Sept. 2017).
20. Chen, X., Dougherty, T., Hong, C., Schibler, R., Zhao, Y. C., Sadeghi, R., Matasci, N., Wu, Y.-C. & Kerman, I. Predicting Antibody Developability from Sequence using Machine Learning. *bioRxiv*. eprint: <https://www.biorxiv.org/content/early/2020/06/20/2020.06.18.159798.full.pdf>. <https://www.biorxiv.org/content/early/2020/06/20/2020.06.18.159798> (2020).
21. Raimondi, D., Simm, J., Arany, A. & Moreau, Y. A novel method for data fusion over entity-relation graphs and its application to protein–protein interaction prediction. *Bioinformatics* **37**, 2275–2281. ISSN: 1367-4803. eprint: <https://academic.oup.com/bioinformatics/article-pdf/37/16/2275/50339388/btab092.pdf>. <https://doi.org/10.1093/bioinformatics/btab092> (Feb. 2021).
22. Wong, L., You, Z.-H., Guo, Z.-H., Yi, H.-C., Chen, Z.-H. & Cao, M.-Y. MIPDH: A Novel Computational Model for Predicting microRNA–mRNA Interactions by DeepWalk on a Heterogeneous Network. en. *ACS Omega* **5**, 17022–17032. ISSN: 2470-1343, 2470-1343. <https://pubs.acs.org/doi/10.1021/acsomega.9b04195> (2024) (July 2020).
23. Gfeller, D., Schmidt, J., Croce, G., Guillaume, P., Bobisse, S., Genolet, R., Queiroz, L., Cesbron, J., Racle, J. & Harari, A. Improved predictions of antigen presentation and TCR recognition with MixMHCpred2.2 and PRIME2.0 reveal potent SARS-CoV-2 CD8+ T-cell epitopes. en. *Cell Systems* **14**, 72–83.e5. ISSN: 24054712. <https://linkinghub.elsevier.com/retrieve/pii/S24054712220004707> (2024) (Jan. 2023).
24. Motmaen, A., Dauparas, J., Baek, M., Abedi, M. H., Baker, D. & Bradley, P. Peptide-binding specificity prediction using fine-tuned protein structure prediction networks. *Proceedings of the National Academy of Sciences* **120**, e2216697120. eprint: <https://www.pnas.org/doi/pdf/10.1073/pnas.2216697120>. <https://www.pnas.org/doi/abs/10.1073/pnas.2216697120> (2023).

25. Weber, A., Born, J. & Rodriguez Martínez, M. TITAN: T-cell receptor specificity prediction with bimodal attention networks. *Bioinformatics* **37**, i237–i244. ISSN: 1367-4803. eprint: https://academic.oup.com/bioinformatics/article-pdf/37/Supplement_1/i237/50694051/btab294.pdf. <https://doi.org/10.1093/bioinformatics/btab294> (July 2021).
26. Fu, T., Huang, K., Xiao, C., Glass, L. M. & Sun, J. HINT: Hierarchical interaction network for clinical-trial-outcome predictions. *Patterns* **3**, 100445. ISSN: 2666-3899. <https://www.sciencedirect.com/science/article/pii/S2666389922000186> (2022).
27. Vu, O., Mendenhall, J., Altarawy, D. & Meiler, J. BCL::Mol2D—a robust atom environment descriptor for QSAR modeling and lead optimization. en. *Journal of Computer-Aided Molecular Design* **33**, 477–486. ISSN: 0920-654X, 1573-4951. <http://link.springer.com/10.1007/s10822-019-00199-8> (2024) (May 2019).
28. Yang, K., Swanson, K., Jin, W., Coley, C., Eiden, P., Gao, H., Guzman-Perez, A., Hopper, T., Kelley, B., Mathea, M., Palmer, A., Settels, V., Jaakkola, T., Jensen, K. & Barzilay, R. Analyzing Learned Molecular Representations for Property Prediction. *Journal of Chemical Information and Modeling* **59**. PMID: 31361484, 3370–3388. eprint: <https://doi.org/10.1021/acs.jcim.9b00237>. <https://doi.org/10.1021/acs.jcim.9b00237> (2019).
29. Boral, N., Ghosh, P., Goswami, A. & Bhattacharyya, M. Accountable Prediction of Drug ADMET Properties with Molecular Descriptors. *bioRxiv*. eprint: <https://www.biorxiv.org/content/early/2022/07/02/2022.06.29.115436.full.pdf>. <https://www.biorxiv.org/content/early/2022/07/02/2022.06.29.115436> (2022).
30. Euclia. <https://github.com/euclia/public-models>. 2023.
31. Boral, N., Ghosh, P., Goswami, A. & Bhattacharyya, M. Accountable Prediction of Drug ADMET Properties with Molecular Descriptors. *bioRxiv*. eprint: <https://www.biorxiv.org/content/early/2022/07/02/2022.06.29.115436.full.pdf>. <https://www.biorxiv.org/content/early/2022/07/02/2022.06.29.115436> (2022).
32. Huang, D., Chowdhuri, S. (, Li, A., Li, A., Agrawal, A., Gano, K. & Zhu, A. *A Unified System for Molecular Property Predictions: Oloren ChemEngine and its Applications* preprint (Chemistry, Oct. 2022). <https://chemrxiv.org/engage/chemrxiv/article-details/6350b9d186473a47d31a8492> (2024).
33. Probst, D., Schwaller, P. & Reymond, J.-L. Reaction classification and yield prediction using the differential reaction fingerprint DRFP. en. *Digital Discovery* **1**, 91–97. ISSN: 2635-098X. <http://xlink.rsc.org/?DOI=D1DD00006C> (2024) (2022).
34. Leenay, R. T., Aghazadeh, A., Hiatt, J., Tse, D., Roth, T. L., Apathy, R., Shifrut, E., Hultquist, J. F., Krogan, N., Wu, Z., Cirolia, G., Canaj, H., Leonetti, M. D., Marson, A., May, A. P. & Zou, J. Large dataset enables prediction of repair after CRISPR–Cas9 editing in primary T cells. en. *Nature Biotechnology* **37**, 1034–1037. ISSN: 1087-0156, 1546-1696. <https://www.nature.com/articles/s41587-019-0203-2> (2024) (Sept. 2019).
35. Kalematis, M., Zamani Emani, M. & Koohi, S. BiComp-DTA: Drug-target binding affinity prediction through complementary biological-related and compression-based featurization approach. en. *PLoS Computational Biology* **19** (ed Schlessinger, A.) e1011036. ISSN: 1553-7358. <https://dx.plos.org/10.1371/journal.pcbi.1011036> (2024) (Mar. 2023).
36. Kinnings, S. L., Liu, N., Tonge, P. J., Jackson, R. M., Xie, L. & Bourne, P. E. A Machine Learning-Based Method To Improve Docking Scoring Functions and Its Application to Drug Repurposing. en. *Journal of Chemical Information and Modeling* **51**, 408–419. ISSN: 1549-9596, 1549-960X. <https://pubs.acs.org/doi/10.1021/ci100369f> (2024) (Feb. 2011).
37. Wei, B. & Gong, X. DeepPLA: a novel deep learning-based model for protein-ligand binding affinity prediction. *bioRxiv*. eprint: <https://www.biorxiv.org/content/early/2021/12/03/2021.12.01.470868.full.pdf>. <https://www.biorxiv.org/content/early/2021/12/03/2021.12.01.470868> (2021).
38. Lam, H. T., Sbodio, M. L., Galindo, M. M., Zayats, M., Fernández-Díaz, R., Valls, V., Picco, G., Ramis, C. B. & López, V. *Otter-Knowledge: benchmarks of multimodal knowledge graph representation learning from different sources for drug discovery* 2023. arXiv: 2306.12802 [cs.LG].
39. Pei, Q., Wu, L., Zhu, J., Xia, Y., Xie, S., Qin, T., Liu, H., Liu, T.-Y. & Yan, R. Breaking the barriers of data scarcity in drug–target affinity prediction. *Briefings in Bioinformatics* **24**, bbad386. ISSN: 1477-4054. eprint: <https://academic.oup.com/bib/article-pdf/24/6/bbad386/54034646/bbad386.pdf>. <https://doi.org/10.1093/bib/bbad386> (Oct. 2023).
40. Lind, A. P. & Anderson, P. C. Predicting drug activity against cancer cells by random forest models based on minimal genomic information and chemical properties. en. *PLoS ONE* **14** (ed Olier, I.) e0219774. ISSN: 1932-6203. <https://dx.plos.org/10.1371/journal.pone.0219774> (2024) (July 2019).
41. Xia, F., Shukla, M., Brettin, T., Garcia-Cardona, C., Cohn, J., Allen, J. E., Maslov, S., Holbeck, S. L., Doroshow, J. H., Evrard, Y. A., Stahlberg, E. A. & Stevens, R. L. Predicting tumor cell line response to drug pairs with deep learning. en. *BMC Bioinformatics* **19**, 486. ISSN: 1471-2105. <https://bmcbioinformatics.biomedcentral.com/articles/10.1186/s12859-018-2509-3> (2024) (Dec. 2018).
42. Preuer, K., Lewis, R. P. I., Hochreiter, S., Bender, A., Bulusu, K. C. & Klambauer, G. DeepSynergy: predicting anti-cancer drug synergy with Deep Learning. *Bioinformatics* **34**, 1538–1546. ISSN: 1367-4803. eprint: https://academic.oup.com/bioinformatics/article-pdf/34/9/1538/48915102/bioinformatics_34_9_1538.pdf. <https://doi.org/10.1093/bioinformatics/btx806> (Dec. 2017).
43. Zheng, S., Rao, J., Zhang, Z., Xu, J. & Yang, Y. Predicting Retrosynthetic Reactions Using Self-Corrected Transformer Neural Networks. en. *Journal of Chemical Information and Modeling* **60**, 47–55. ISSN: 1549-9596, 1549-960X. <https://pubs.acs.org/doi/10.1021/acs.jcim.9b00949> (2024) (Jan. 2020).